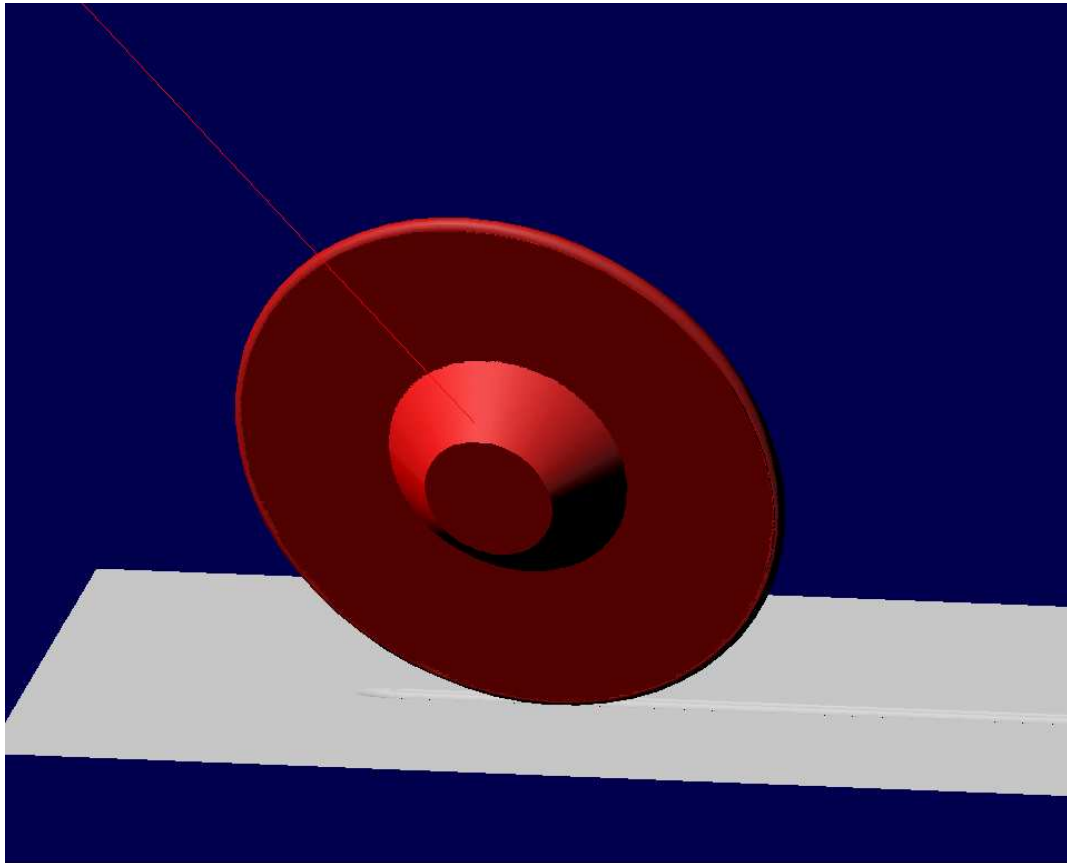


CHALMERS



Adams modelling of contact forces between disc cutter and mount

Master's Thesis in the Master's programme Solid and Fluid Mechanics

ANDERS ERICSSON

Department of Applied Mechanics
Division of Dynamics
CHALMERS UNIVERSITY OF TECHNOLOGY
Göteborg, Sweden 2010
Master's Thesis 2010:30

MASTER'S THESIS 2010:30

Adams modelling of contact forces
between disc cutter and mount

Master's Thesis in the Master's programme Solid and Fluid Mechanics

ANDERS ERICSSON

Department of Applied Mechanics
Division of Dynamics
CHALMERS UNIVERSITY OF TECHNOLOGY
Göteborg, Sweden 2010

Adams modelling of contact forces between disc cutter and mount

Master's Thesis in the Master's programme Solid and Fluid Mechanics
ANDERS ERICSSON

© ANDERS ERICSSON, 2010

Master's Thesis 2010:30
ISSN 1652-8557
Department of Applied Mechanics
Division of Dynamics
Chalmers University of Technology
SE-412 96 Göteborg
Sweden
Telephone: + 46 (0)31-772 1000

Cover:
Disc cutter penetrating into the rock surface.

Department of Applied Mechanics
Göteborg, Sweden 2010

Adams modelling of contact forces between disc cutter and mount

Thesis in the Master's programme Solid and Fluid Mechanics

ANDERS ERICSSON

Department of Applied Mechanics

Division of Dynamics

Chalmers University of Technology

ABSTRACT

The purpose of this thesis has been to develop a calculation module for use in the simulation software Adams. The calculation module is based on equations found in the literature. A disc cutter is the tool in contact with the mount for example in tunnel boring machines. A disc cutter is a circular disc, made of high strength steel. A literary study was made where equations determining the forces acting on the disc cutter were found. The equations used in the module are based on the disc cutter's penetration into the rock, the spacing between two cuts and the rock properties, such as the compressive and Brazilian tensile strength. The simulation module was made and used in the simulation software Adams where the forces and moments acting on the disc cutter while cutting rock can be simulated. The advantage of the simulation model is that it is built in such a way that many disc cutters can be linked together and the forces from each of them can work together. A test was made on the simulation model and compared to a real test from the literature, made in a Linear Cutting Machine, and the theoretical calculated force from the model for the given rock penetration and spacing between the two cuts. The simulation model showed a clear correlation to the theoretical calculated normal force, the normal force from the LCM test was higher. The rolling force from the theoretical model correlated well to the rolling force from the LCM test while the simulation generated a higher rolling force. The side forces for the LCM test and the simulation model correlated well.

Key words: Disc cutter, tunnel boring machine, Adams, cutter force, simulation

Adams-modellering av kontaktkraften mellan cutter och berg

Examensarbete inom Solid and Fluid Mechanics

ANDERS ERICSSON

Institutionen för tillämpad mekanik

Avdelningen för Dynamik

Chalmers tekniska högskola

SAMMANFATTNING

Syftet med detta arbete har varit att skapa en beräkningsmodul att använda i simuleringsprogrammet Adams. Beräkningsmodulen baseras på ekvationer funna i litteraturen. En cutter är verktyget som är i kontakt med berget i till exempel en tunnelbormaskin. Cuttern är en rund skiva, gjord av höghållfast stål. En litteraturstudie gjordes där ekvationer som beskriver krafterna som agerar på cuttern hittades. De ekvationer som används i modulen är baserade på cutterns penetrering i berget, avståndet i sidled mellan två cuttrar och bergets egenskaper, tryckhållfastheten och den brasilianska draghållfastheten. Simuleringsmodellen har byggts i simuleringsprogrammet Adams där de krafter och moment som agerar på cuttern när den penetrerar berget kan simuleras. Fördelen med denna simuleringsmodell är att den kan simulera många cuttrar tillsammans, där krafter och moment på var och en av dem arbetar tillsammans. Ett test har gjorts där krafter från simuleringsmodellen jämförts med de teoretiska krafterna och krafterna från ett riktigt test beskrivet i litteraturen, gjort i en Linear Cutting Machine, LCM. Normalkraften från den teoretiska modellen stämde mycket väl överens med normalkraften från simuleringsmodellen medan normalkraften från det verkliga testet var något högre. Rullkraften från den teoretiska modellen stämde väl överens med rullkraften från LCM-testet medan simuleringen gav en högre rullkraft. Sidokrafterna från LCM-testet och simuleringsmodellen korrelerade väl.

Nyckelord: Cutter, tunnelbormaskin, Adams, cutterkraft, simulering

Contents

ABSTRACT	I
SAMMANFATTNING	II
CONTENTS	III
PREFACE	VII
NOTATIONS	VIII
1 INTRODUCTION	1
1.1 Background	1
1.2 Purpose	1
1.3 Limitations	1
2 ROCK FRAGMENTATION BY DISC CUTTING	2
2.1 Introduction to the rock cutting process	2
2.2 Performance prediction models	3
2.3 Rock mechanics	4
2.3.1 Crushed zone	4
2.3.2 Compacted zone	4
2.3.3 Cracked zone	5
2.3.4 Chipping procedure	5
2.3.5 Spacing	5
2.4 Cutting speed	6
2.5 Linear cutting machine	7
2.6 Specific energy	8
2.7 Cutter types	8
3 FORCE ESTIMATION MODELS	11
3.1 Introduction	11
3.2 Cutter forces	11
3.2.1 Force estimation methods	11
3.2.2 Non-loading zones	15
3.3 Cutter force model	16
4 SIMULATION TOOLS	18
4.1 Adams	18
4.2 Markers	18
4.3 Joints	19
4.4 Forces	19

4.4.1	General force	19
4.5	Adams solver	19
5	VIRTUAL TUNNEL FACE	21
5.1	Introduction	21
5.2	Modelling the tunnel face	21
5.3	Elements	23
5.3.1	Lower element	24
5.3.2	Upper element	25
6	CUTTER GEOMETRY	27
6.1	Coordinate systems	27
6.2	Coordinate system transformations	28
6.3	Cutter edge	30
7	FORCE CALCULATION	32
7.1	Introduction	32
7.2	Force calculations in Adams	32
7.3	Penetrated plane	33
7.4	Normal vector	33
7.5	Penetration	38
7.6	Friction	39
7.6.1	Velocity	39
7.6.2	Friction coefficient	41
7.7	Cutter force	41
7.8	Cutter moment	42
8	ROCK FRAGMENTATION	43
8.1	Deformation	43
8.2	Matrix update	44
8.2.1	Temporary rock matrix	45
9	MODEL VALIDATION	46
9.1	Inputs	46
9.2	Theoretical force	47
9.3	Simulation force	48
9.4	Comparison	51
10	MODEL LIMITATIONS	52

10.1	Detecting penetration	52
10.2	Penetrated plane	52
10.3	Chipping	52
11	DISCUSSION AND RESULTS	53
12	FUTURE WORK	54
13	REFERENCES	55

Preface

In this study, a simulation model has been constructed in which the contact forces between a disc cutter and mount can be studied. The Master Thesis was initiated by Atlas Copco Rock Drills AB and the work has been carried out at their office in Örebro.

I would like to thank my supervisor Morgan Norling for all the support, discussions and encouragement throughout the work. A special thanks also to my examiner and supervisor at Chalmers, Per-Åke Jansson. I would also like to thank Atlas Copco Rock Drills AB, Kenneth Weddfelt and Lars Persson for financing, facilities, material and guidance.

Örebro, May 2010

Anders C W Ericsson

Notations

Roman upper case letters

$A_{element}$	Element area
C	Constant
F_{fr}	Friction force
F_n	Normal force
F_r	Rolling force
F_T	Cutter force
F_{tot}	Total force
F_x	Force in the x-direction
F_x'	Force in the x-direction in the local coordinate system
F_y	Force in the y-direction
F_y'	Force in the y-direction in the local coordinate system
F_z	Force in the z-direction
H	Height
K	Node number in y-direction
L	Node number in x-direction
L_f	Length
M_{tot}	Total moment
N	Normal vector
P'	Base pressure
R	Cutter radius
R_z	Transformation matrix
$R_{y'}$	Transformation matrix

R_x	Transformation matrix
S	Spacing between cuts
T	Cutter tip thickness
\underline{TVEL}	Translational velocity
T_x'	Moment around the local x-axis
T_y'	Moment around the local y-axis
T_z'	Moment around the local z-axis
$VREF$	Velocity vector

Roman lower case letters

\underline{c}	Centre of disc cutter
c_{\max}	Maximum damping coefficient
d	Penetration for when full damping is applied
d_{fr}	Direction of the friction force
\underline{d}_p	Vector
dx	Element length in the x-direction
dy	Element length in the y-direction
e	Exponent
\underline{e}_n	Element normal vector
\underline{f}_p	Distance vector
k	Stiffness
kk_x	Start node number in the x-direction
kk_y	Start node number in the y-direction
k_{x1}	Lowest node number in the actual element in the x-direction

k_{x2}	Highest node number in the actual element in the x-direction
k_{y1}	Lowest node number in the actual element in the y-direction
k_{y2}	Highest node number in the actual element in the y-direction
l	Length
n_x	X-component of normal vector
n_y	Y-component of normal vector
n_z	Z-component of normal vector
p	Cutter penetration
$\underline{p_1}$	Point
$\underline{p_c}$	Centre of penetrated plane
<i>penetration</i>	Penetration depth
r	Radius
\underline{r}	Distance vector
<i>rockdx</i>	Element length in x
<i>rockdy</i>	Element length in y
$rockx_{\min}$	Coordinate node one in x
$rockx_{\max}$	Coordinate last node in x
$rocky_{\min}$	Coordinate node one in y
$rocky_{\max}$	Coordinate last node in y
<i>rockz</i>	Rock surface matrix
<i>stepz</i>	Parameter
$\underline{s_m}$	Cutter force
t	Variable
<i>trockz</i>	Temporary rock surface matrix

$vector_{one}$	Vector
$\underline{s}_{pl,1}$	Direction vector for the penetrated plane
$\underline{s}_{pl,2}$	Direction vector for the penetrated plane
\underline{v}_{pl}	Velocity vector
v_{fr}	Friction velocity
\underline{v}_{fr}	Friction velocity vector
v_x'	Velocity x-direction in the local coordinate system
v_y'	Velocity y-direction in the local coordinate system
\underline{v}_2	Vector
\underline{v}_1	Vector
x	Coordinate in the x-direction
x_{coord}	X-coordinate
x_{disc}	X-coordinate
x_{dist}	Distance in x-direction
x_f	X-coordinate
x_{local}	Local x-coordinate
$x_{local,edge}$	Local x-coordinate on the disc cutter edge
x_m	Actual position of the centre of the element in the x-direction
x_{min}	Coordinate of node one in the x-direction
\dot{x}	Time derivative of x
x_1	Distance in the global y-direction for when the wheel gets in contact with ground
x'	X-component in the new local coordinate system
y	Coordinate in the y-direction

y_{coord}	Y-coordinate
y_{disc}	Y-coordinate
y_{dist}	Distance in y-direction
y_f	Y-coordinate
y_{local}	Local y-coordinate
$y_{local,edge}$	Local y-coordinate on the disc cutter edge
y_m	Actual position of the centre of the element in the y-direction
y_{min}	Coordinate of node one in the y-direction
y'	Y-component in the new local coordinate system
$z_{coord,wheel}$	Z-coordinate on the edge of the wheel
$z_{coord,wheelcentre}$	Z-coordinate in the wheel centre
z_{disc}	Z-coordinate
z_f	Z-coordinate
z_{mean}	Mean z-value
z_{rock}	Rock surface matrix
z'	Z-component in the new local coordinate system
$z_{l,p1}$	Z-coordinate
$z_{l,p2}$	Z-coordinate
z_{local}	Local z-coordinate
$z_{local,edge}$	Local z-coordinate on the disc cutter edge

Greek upper case letters

Φ	Angle of the part in contact with the rock
Δv	Difference in velocity

Θ Angle

Greek lower case letters

α Angle to the point of interest

β Angle

ω_z Angular velocity around the z-axis

$\underline{\omega}$ Angular velocities

μ Friction coefficient

σ_c Uniaxial compression strength of rock

σ_t Brazilian tensile strength of rock

γ Angle from the x-axis of the new coordinate system to the total force

ψ Exponent of the pressure distribution function

θ Angle from the normal to the point of interest

1 Introduction

1.1 Background

As the infrastructure projects are getting larger and roads and railways are expanding, the greater the tunnelling industry gets. There are two main disciplines of building tunnels in rock. Either the tunnel is built through drill and blast or by different types of tunnel boring machines. Tunnel boring machines have plenty of advantages, they are fast and safe as long as the profile of the tunnel is the same.

In the front of the tunnel boring machine there are disc cutters that are in contact with the rock. To be able to make the tunnel boring machines faster, and to reduce the damage on the machine, the machine performance needs to be optimized and the machine needs to be designed to withstand the different forces acting on it. To do that, the forces acting on the front part of the machine from the rock needs to be known.

1.2 Purpose

Computer simulations are a good way to reduce time and costs during the development of new tunnel boring machines. The purpose with this master thesis is to build a simulation model of the rock cutting using disc cutters, which can be used to study the contact forces between the disc cutter and the mount.

The forces acting on the disc cutter are hard to calculate exactly and a completely true simulation model of the rock fragmentation process is hard to make. There are many force estimation models to use to calculate the cutting forces from a known penetration depth, which will be used in this master thesis to simulate the rock cutting.

1.3 Limitations

A model of the disc cutting should be developed in the mechanical simulation software Adams, which is used by Atlas Copco AB. The model should be constructed such that many different disc cutters can be linked together and that the forces acting on each disc cutter can be summed to a total force.

2 Rock fragmentation by disc cutting

2.1 Introduction to the rock cutting process

Tunnel boring machines are the most frequently used machines in the tunnelling industry. The reason for the extensive use of tunnel boring machines is the large amount of advantages it has. The tunnel boring machine is fast, safe and it works well in different ground conditions as long as the profile of the tunnel is kept constant. Disc cutters can be used in the front of a tunnel boring machine, see Figure 1.



Figure 1 A tunnel boring machine with disc cutters. Gertsch et al (2002)

A disc cutter is a disc made of high strength steel that rolls against the rock with thrust force acting on it. A number of disc cutters are mounted on a big drum, the drum is rotating and a thrust is added to it, and a tunnel boring machine is created. The diameter of the drum can be very large, it depends on the strength of the rock and the number of disc cutters needed. Since the machine only can produce a given thrust force and the torque of the machine is limited, the number of disc cutters possible to use is limited. The total thrust force is the sum of the thrust force on each disc cutter.

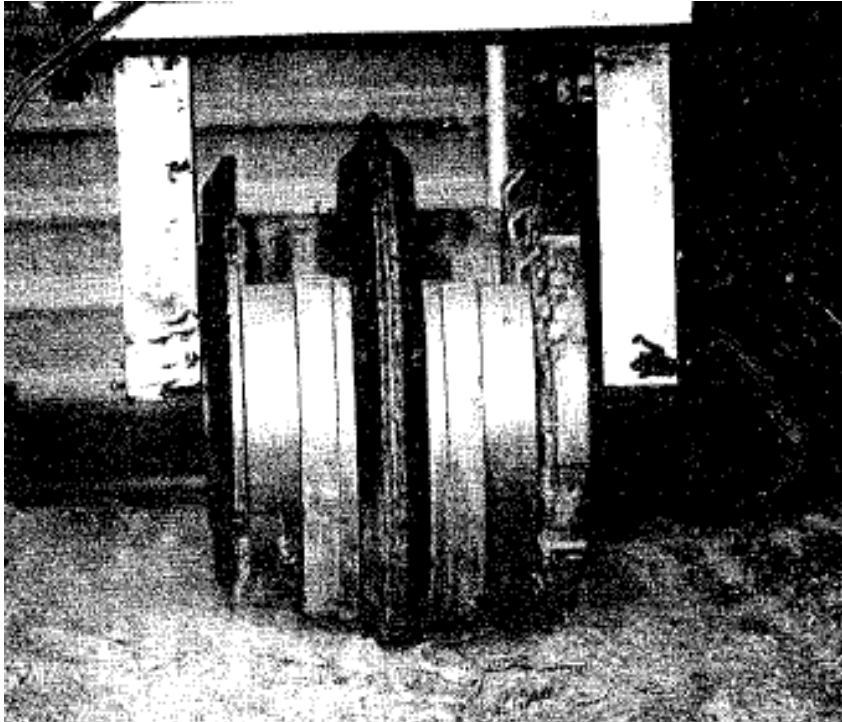


Figure 2 Example of a disc cutter. Lindqvist et al (1980)

When a disc cutter is rolling against the rock a reaction force from the rock is acting on the disc cutter. This force is then divided into two components, called the normal and rolling forces. The normal force is the thrust force and the rolling force is the force in the rolling direction. The rolling force multiplied with the distance to the centre of the drum will create a rotational moment. The maximum value of that moment is the torque available in the machine. An example of a disc cutter cutting rock can be seen in Figure 2.

2.2 Performance prediction models

Many performance prediction models have been presented where the force acting on the disc cutter has been a function of the cutter penetration, e.g. Sanio (1985), Snowdon et al (1982) and Ozdemir and Rostami (1993). In these studies the number of disc cutters and the spacing to penetration ratio have been optimized. The force acting on the disc cutter or the specific energy has been studied as a function of the spacing to penetration ratio and by using that an optimum spacing to penetration ratio has been achieved. The specific energy is the energy needed for cutting a specific volume of the rock. Therefore the specific energy is a good way of measuring the cutting efficiency. When measuring the specific energy during rock cutting with disc cutters the horizontal, or the rolling, force is used to calculate the energy. Since the penetration is rather small in comparison with the length of the cut the energy from the normal force can be neglected.

In the performance models the performance of the tunnel boring machine will be calculated as a function of the thrust and power available in the machine for rock cutting. By using this information together with the calculated forces that will act on the disc cutter while cutting, a rate of penetration can be calculated for the specific

tunnel boring machine. The rate of penetration is usually expressed in terms of m^3/h of excavated rock volume or m/h , the tunnel length bored per hour.

2.3 Rock mechanics

2.3.1 Crushed zone

During rock cutting with disc cutters, a zone with highly fractured rock will appear just beneath the cutter. This zone is called the crushed zone and is caused by the high stress concentrations from the edges of the disc cutter geometry. Since the fragments are very fine grained, the area of new surfaces created during the fragmentation process is very large. This means that the creation of the crushed zone is very energy consuming. If the size of the crushed zone instead is small, less energy will be needed to create it and the energy can be used for side chipping. The different zones in the rock during the rock cutting process can be seen in Figure 3.

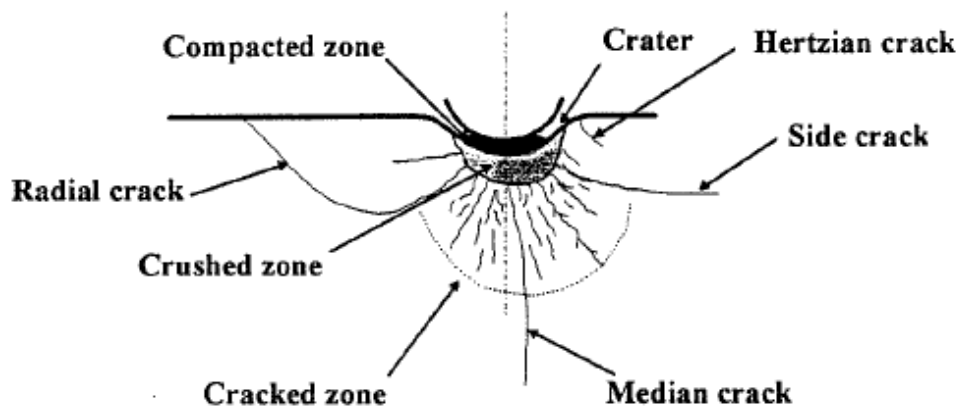


Figure 3 The different zones occurring during indentation in the rock. Shaoquan (1995)

The crushed zone is assumed to have a shape of a half ellipsoid with the shortest diameter in the direction of the loading and the largest diameter parallel to the cut, since the measurement is not truly possible to make. The width of the crushed zone is assumed to be approximately 1.2 – 1.3 times the tip width and the depth of the crushed zone is proportional to the penetration depth. The tip width is the width of the cutter tip, see Figure 9.

2.3.2 Compacted zone

There occurs a zone of compacted rock above the crushed zone during the chipping process rather than the stable penetration process. This is because the rock powder is trapped in between the disc cutter and the crater walls and when it is compressed it is formed to a new material with properties almost the same as the intact rock material, Lindqvist (1982). This process has a negative influence on the cutting process, even if the amount of energy used for this is not that large.

2.3.3 Cracked zone

Underneath the crushed zone a zone with highly cracked rock will appear. This zone is called the cracked zone. The size of the cracked zone varies with the load magnitude and the macro mechanical properties of the rock, Shaoquan (1995).

2.3.4 Chipping procedure

During rock cutting with disc cutters rock chips are created. This phenomenon is not completely investigated and an exact theoretical explanation is not available. Chipping is supposed to occur at the front non-loading zone, Gertsch et al (2002). The front non-loading zone can be seen in Figure 11 and is described in Chapter 3.2.2. When the pressure in the crushed zone is high enough a rock chip is created. There are two cases for rock chipping, the first is that the crack meets a free surface and therefore forms a chip. The second case is that the crack meets an adjacent crack created by another disc cutter from an earlier cut and a large chip is created. The adjacent crack can also be in the rock from the beginning. Exactly when and in what direction the crack will propagate is not known, but usually it propagates in the weakest direction or where the stresses in the rock are the largest. The rock chipping and the chips created can be seen in Figure 4.

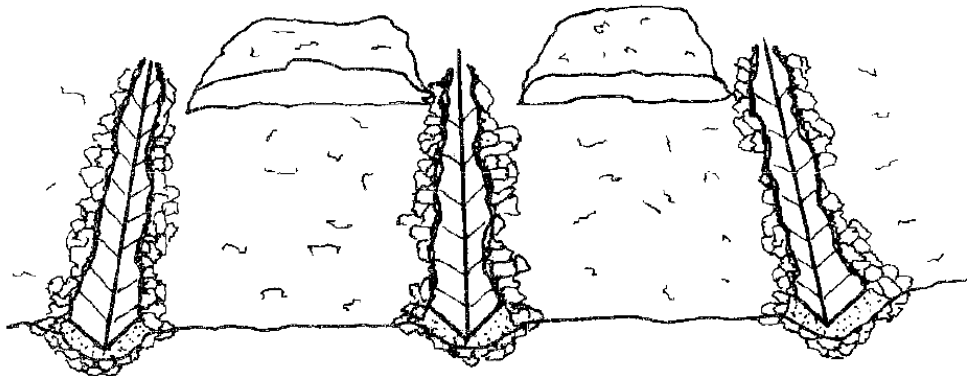


Figure 4 Chips and crushed rock during disc cutting. Lindqvist et al (1980)

2.3.5 Spacing

The distance between the disc cutters sideways is called the disc cutter spacing. The disc cutter spacing plays an important role in the rock fragmentation process. The force needed for the rock fragmentation can be reduced if the spacing between the cuts can be optimized. Normally the S/P-ratio, spacing to penetration, is between 10 and 20. This value depends on the disc cutter type and the rock type that the cut will be made in. A typical curve of the specific energy as a function of the S/P-ratio with the optimum S/P-ratio can be seen in Figure 5.

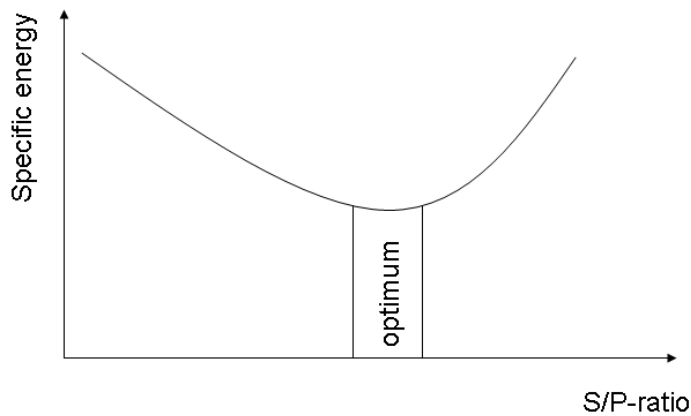


Figure 5 Typical optimum S/P-ratio curve

When the distance between two cuts is too large or when the pressure in the crushed zone is too low to generate a chip a ridge is formed. That is when the rock material between the cuts is still there and not chipped out. If the force instead is too high the chips created can be thicker than the penetration depth. The optimum spacing between two adjacent cuts is instead the distance when the cracks propagate straight to the neighbouring crack and forms a chip. The shorter the crack propagation path is the less energy is needed, Ozdemir et al (1993).

2.4 Cutting speed

The cutting speed has minimal influence on the cutting forces acting on the disc cutter. The same behaviour has been seen also for the yield and specific energy during rock cutting. Yield is the volume of rock excavated by the disc cutter per unit length of cut. This can be seen in Figure 6.

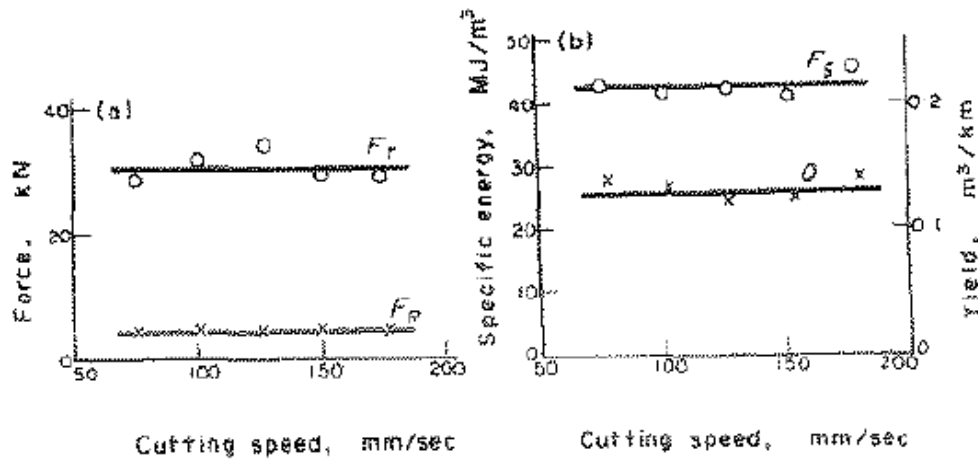


Figure 6 The rolling and normal force and the specific energy as a function of the cutting speed. Roxborough (1975)

When the cutting speed is of the same order of magnitude as the crack propagation rate of rock then there are some noticeable effects, Roxborough and Phillips, (1975). Gertsch et al (2002) made several tests on Colorado Red Granite where they investigated the dynamic behaviour of rock fragmentation with disc cutters. They noticed that increasing the spacing and the penetration decreases the dynamic range of the forces acting on the disc cutter. The larger the spacing and penetration is, the smaller the deviation from the mean force will be.

The force will have a shape as a saw tooth function during disc cutting. This is because of the chipping process, when chipping occurs the pressure in the crushed zone will decrease and therefore the force acting on the cutter will decrease and the force can be described as a saw tooth. Gertsch et al (2002) also found that the number of chips created during a cut is independent of the cutter velocity. The behaviour of the saw tooth shaped force is dependent on the strength of the rock, the stronger the rock is the higher the amplitude of the variation will be and the shorter the period will be. For a weak rock it is the other way around, low amplitude and a long period.

2.5 Linear cutting machine

Most of the laboratory work in this area is carried out in a linear cutting machine, LCM. An LCM is a machine that can roll a disc cutter in original size against the rock with a controlled thrust or with a specific penetration depth. The cutting speed can be controlled in the LCM rig, so also the spacing between the cuts, Nilsen et al (1993). One can study the influence of all the different parameters affecting the cutting efficiency by using the LCM. An example of a linear cutting machine can be seen in Figure 7.

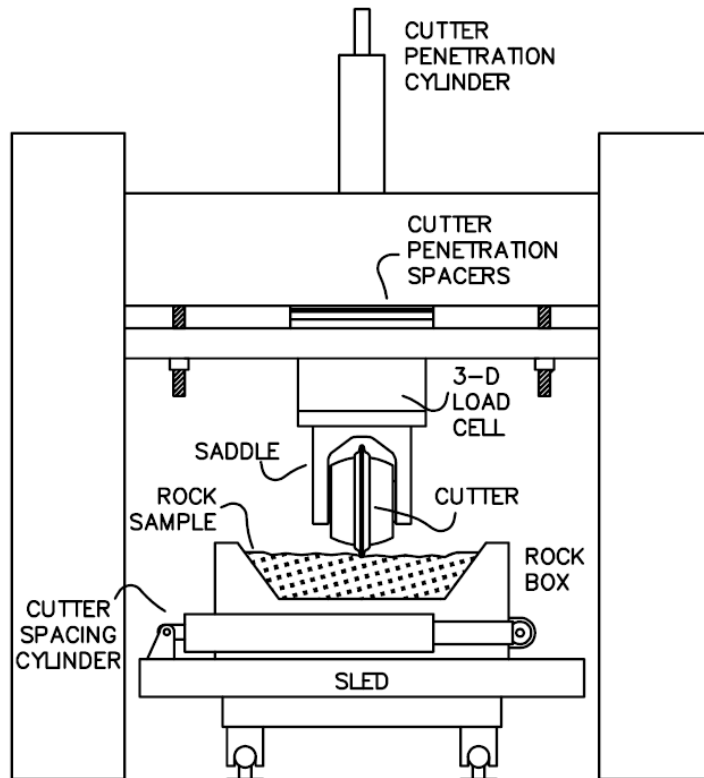


Figure 7 An example of a linear cutting machine. Rostami (1997)

The size of the rock block that the disc cutter rolls against in the LCM is limited. Therefore the cuts closest to the edges are abandoned due to the side effects. From the results from the LCM different force estimation models can be obtained. These are discussed in Chapter 3.

2.6 Specific energy

One of the most common things to study, in for example linear cutting tests, is the specific energy. The specific energy is the energy needed to excavate a specific rock volume and is a measurement of the cutting efficiency. If the specific energy is low the energy needed to excavate a unit volume of rock is low. The specific energy is normally calculated as the energy during one cut divided by the excavated rock volume. The energy needed during the cut is the work done by the two force components, the normal and rolling force. Since the length of the cut is much larger than the penetration depth the work by the normal force can be assumed to be negligible.

2.7 Cutter types

There are many different types of disc cutters used. One type of disc cutters has inserted buttons of high strength metal, see Figure 8. But the most common type is the constant cross section disc cutter (CCS) which will be used in this model.



Figure 8 Disc cutter with inserted buttons. Lindqvist (1982).

As mentioned above the most common type of disc cutter is the CCS cutter. The cutter that will be used in this model is a CCS cutter and can be seen in Figure 9 together with the measures.

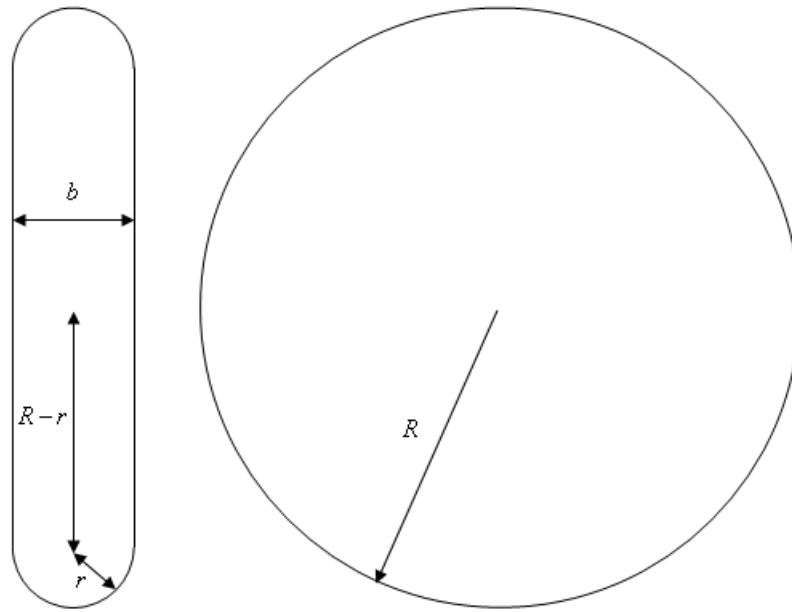


Figure 9 The disc cutter from a cross sectional view and viewed from the side with the measures

3 Force estimation models

3.1 Introduction

There is no simple explanation of the behaviour of the rock fragmentation process under a disc cutter. Many attempts have been made trying to find out all the mechanisms involved in the rock fragmentation process under a disc cutter. What is known is that a crushed zone will appear beneath the tip of the cutter because of a high pressure concentration from the cutter tip, Rostami and Ozdemir (1993) and Lindqvist (1982). The exact pressure distribution in this zone is not known but it is assumed to be circular, Rostami and Ozdemir (1993). The size of this zone needs to be small in order to get a highly efficient cut, since it requires a great deal of energy to crush the rock into small pieces instead of creating larger chips of the rock. Because of the formation of microcracks in the crushed zone, there will be a volumetric expansion in the crushed zone. This expansion will cause tensile stresses which will give rise to tensile crack propagation to the surface to form rock chips, Hongyuan (2003). When a chip comes into being, the pressure in the crushed zone decreases which leads to an oscillation in the force acting on the cutter, Sanio (1985).

3.2 Cutter forces

3.2.1 Force estimation methods

The following part, Chapter 3.2.1, is taken from Ozdemir and Rostami (1993) and it presents a model for the forces acting on the cutter as a function of penetration and rock type. In this model, the stress is supposed to be distributed as:

$$P = P' \left(1 - \frac{\theta}{\Phi} \right)^\psi \quad (1)$$

where

- P' Base pressure
- θ Angle from the normal to the point of interest
- Φ Angle of the part in contact with the rock
- ψ Exponent of the pressure distribution function

The angles can be seen in Figure 10.

The exponent of the pressure distribution determines the shape of the pressure distribution, a value of $\psi = 0$ means a uniform pressure distribution along the cutter edge. For a pressure distribution starting from zero in the front of the disc cutter and P' under, $\psi = 1$ is used. A negative value of ψ means higher pressure in the front of the disc cutter. Ozdemir and Rostami, (1993)

The base pressure is calculated from test data from different tests made with an LCM (linear cutting machine) on several rock types and conditions. From these tests three different equations for calculating the base pressure are presented, depending on how many parameters that are known. The most accurate method is the third and it depends on the compression and tensile strength of the rock, the cutter radius, the spacing between the different cuts, the penetration and the thickness of the cutter. The third method has a square of the correlation coefficient of 0.865, the second has a square of the correlation coefficient of 0.78 and the first has a square of the correlation coefficient of 0.525. The pressure functions are, equation (2) to (4):

$$P'_1 = -32628 + 521\sigma_c^{0.5} \quad (2)$$

$$P'_2 = 103400 + 4200S - 7.37\sigma_t + 2.48\sigma_c - 1260p - 21030T - 11740R \quad (3)$$

$$P'_3 = 100500 + 12170S + 7.88\sigma_c - 28830\sigma_t^{0.1} - 192S^3 - 0.000147\sigma_c^2 - 29450T - 13000R \quad (4)$$

where

σ_c Uniaxial compression strength of rock [psi]

σ_t Brazilian tensile strength of rock [psi]

S Spacing between cuts [in]

T Cutter tip thickness [in]

R Cutter radius [in]

p Penetration [in]

$P'_1 - P'_3$ Pressure on the brim

This model is valid for the following values of the variables, according to Table 1.

Table 1 The limit values for the force model

Variable	Lower limit	Upper limit	Unit
σ_c	10000	30000	psi
σ_t	500	2500	psi
R	15	18	in
S	2	4	in
p	0.25	3	in

The total force acting on the cutter can be seen in Figure 10 and is calculated according to

$$F_i = \frac{P' RT\Phi}{\psi + 1} \quad (5)$$

where

- P' Base pressure [psi]
- R Cutter radius [in]
- T Cutter tip thickness [in]
- Φ Angle of the part in contact with the rock
- ψ Exponent of the pressure distribution function

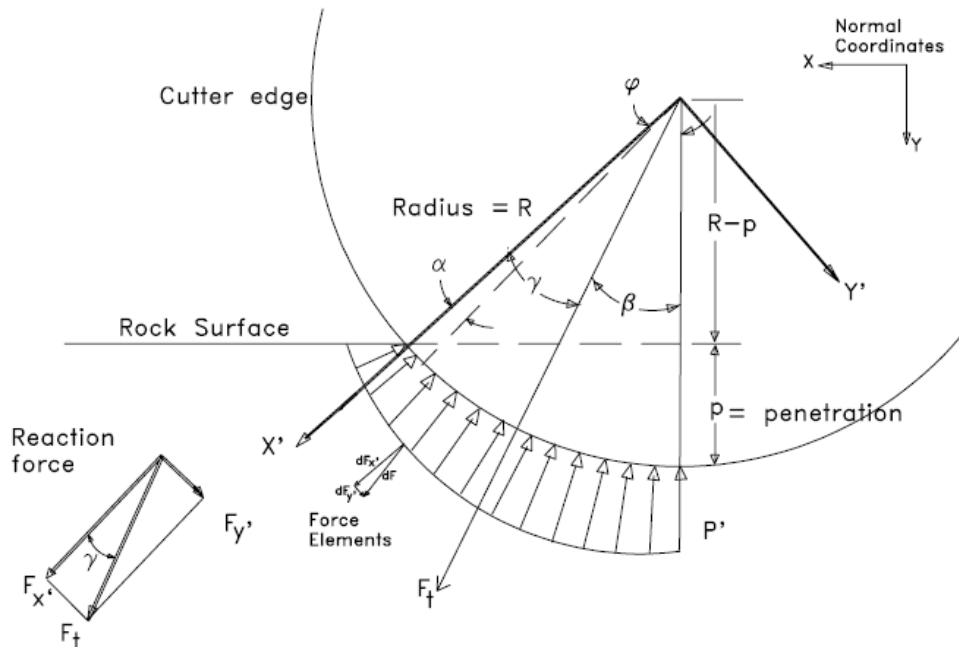


Figure 10 The stress distribution. Gertsch et al (2002)

To be able to describe the base pressure under the cutter in a more general way a new angle is introduced to determine the pressure at any point in contact with the rock. The equation for the pressure distribution in a general way using a power function is described in equation (6):

$$P = P' \left(\frac{\alpha}{\phi} \right)^\psi \quad (6)$$

Where

α Angle to the point of interest

The force component at any angle α of interest can be calculated as

$$dF = TRP d\alpha = TRP' \left(\frac{\alpha}{\phi} \right)^\psi d\alpha = TRP' \phi t^\psi dt \quad (7)$$

where

t Variable replacing $\frac{\alpha}{\phi}$

The force components in the x- and y-directions in the new coordinate system are calculated as equations (8) and (9):

$$F_{x'} = \int_0^\phi dF_{x'} = \int_0^\phi dF \cos(\alpha) \quad (8)$$

$$F_{y'} = \int_0^\phi dF_{y'} = \int_0^\phi dF \sin(\alpha) \quad (9)$$

The angle from the x-axis of the new coordinate system to the axis of the total force is then calculated from

$$\gamma = \tan^{-1} \left(\frac{F_{y'}}{F_{x'}} \right) \quad (10)$$

where

γ Angle from the x-axis of the new coordinate system to the total force

Ozdemir and Rostami (1993) also present equations to calculate the normal and rolling forces on the cutter. The equations for the rolling and normal forces calculated according to equations (11) and (12).

$$F_n = F_t \cos(\beta) \quad (11)$$

$$F_r = F_t \sin(\beta) \quad (12)$$

where

F_n Normal force

F_r Rolling force

3.2.2 Non-loading zones

During investigations, Rostami (1997), the stress distribution on the disc cutter is found out not to be hydrostatic. Instead there is a non-loading zone in the front and in the rear of the contact zone on the disc cutter, Rostami (1997). Tests have been done where strain gauges were mounted on the disc cutter while doing linear cuts with a linear cutting machine which showed that the stress only acts on a limited area on the disc cutter. There is a non-loading zone in the front and in the rear of the area in contact with the rock. The front non-loading zone is assumed to appear because of the chipping procedure in front of the disc cutter. The rear non-loading zone depends on the removal of crushed material from the back of the cutter, Rostami (1997) and Gertsch et al (2002). The pressure distribution on the disc cutter can be seen in Figure 11.

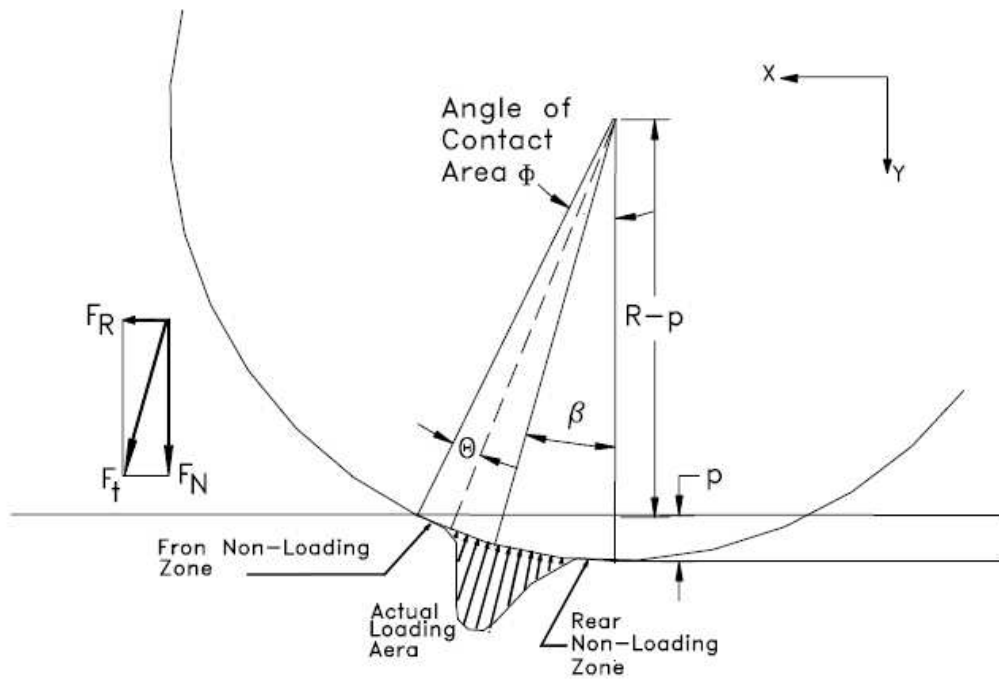


Figure 11 The pressure distribution on the disc cutter in the method presented by Rostami (1997). Gertsch et al (2002)

3.3 Cutter force model

Based on the above mentioned stress distribution, see Figure 11, a complete series of regression analysis have been made on several test data obtained from tests on a linear cutting machine, LCM. The results have been analyzed and the correlation between cutting forces and different rock parameters has been studied. The result from these analyses is the following force equations. This force model is different from the force model by Ozdemir and Rostami (1993), since it takes the actual loading area into consideration.

The normal force acting on the disc cutter according to Figure 11 is as follows, Gertsch et al (2002), equation (13).

$$F_N = TR\phi P' \cos\left(\frac{\phi}{2}\right) \quad (13)$$

where

- F_N Normal force [N]
- T Tip thickness of the cutter [m]
- R Cutter radius [m]
- ϕ Angle of the contact area

P' Average pressure in the contact area [Pa]

The angle of the contact area is calculated as

$$\phi = \cos^{-1}\left(\frac{R-p}{R}\right) \quad (14)$$

where

p Cutter penetration [m]

The mean pressure in the loading area is calculated as

$$P' = C\sqrt[3]{\frac{\sigma_c^2 \sigma_t S}{\sqrt{RT}}} \quad (15)$$

where

$C = 2.12$ is a constant

The rolling force is the horizontal component of the force acting on the disc cutter. The rolling force is calculated using the cutting coefficient, which means how much of the force that is used for the rolling. The rolling force is calculated according to equation (16). The location of the actual loading area, see Figure 11, depends on the rock properties and penetration depth. It can in a general case be set to half of the angle of the contact area.

$$F_R = F_N \tan\left(\frac{\phi}{2}\right) \quad (16)$$

One can therefore say that resultant force that will act on the edge of the disc cutter in contact with the rock will be

$$F_t = TR\phi P' \quad (17)$$

Equation (17) will be used later in the report for calculating the cutter forces.

4 Simulation tools

4.1 Adams

Adams, Automatic Dynamic Analysis of Mechanical Systems, mechanical simulation software is used in this Master Thesis. Adams is a software used to simulate Multi Body Systems (MBS). A Multi Body System consists of parts, rigid or flexible, that are linked together by joints and/or force elements. Adams can be used to simulate flexible bodies, but a standard Adams part is rigid and can not be deformed. Each part has six degrees of freedom, three translational and three rotational. An example of an MBS with bodies, joints and forces can be seen in Figure 12.

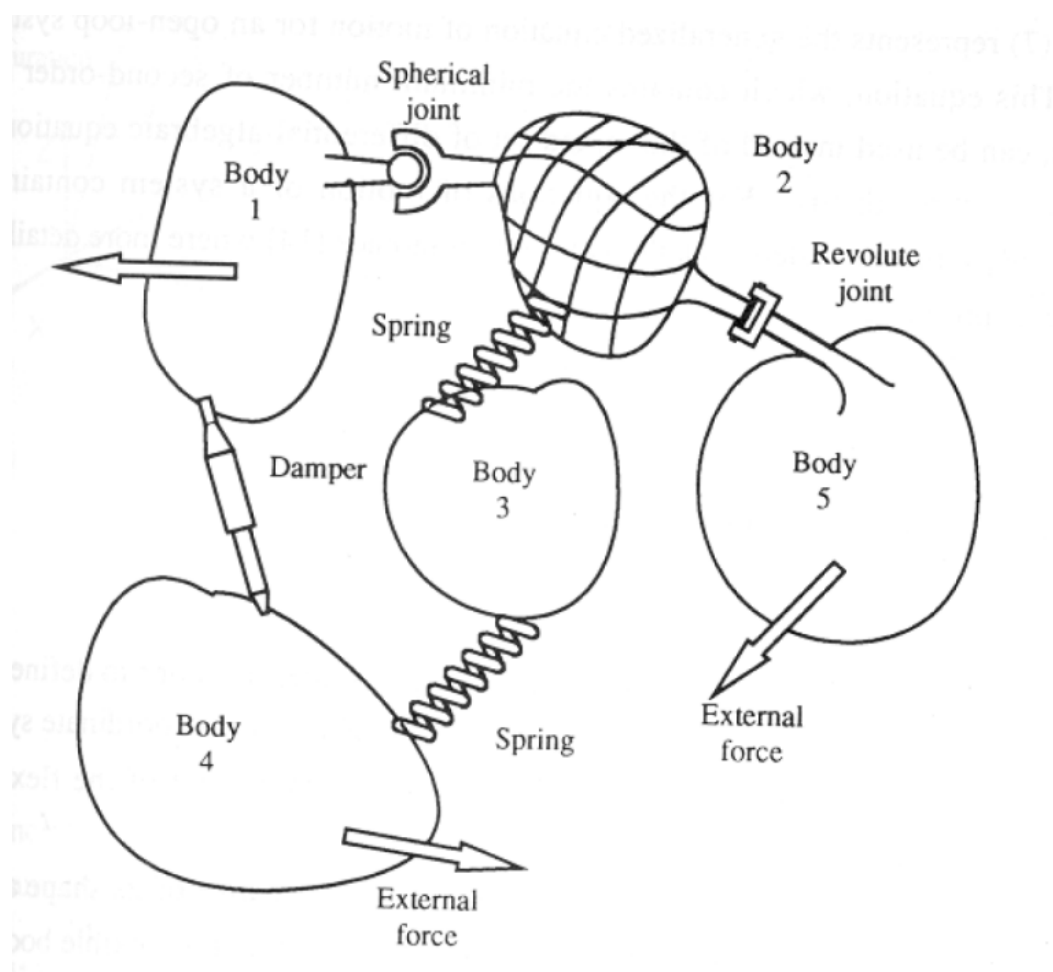


Figure 12 Example of a multi body system with joints and forces

4.2 Markers

A marker is a coordinate system and is used in Adams whenever a certain direction or position needs to be specified. It can for example specify where a geometry needs to be anchored to the part or where the centre of mass of the part is. When building a model, a marker defining the global origin will always be attached. This marker also

defines the global directions. All new markers will automatically have their positions and directions expressed in the global reference system.

4.3 Joints

A joint is a connection between two parts in ADAMS that constrains 1-6 degrees of freedom. There are many different types of joints. A revolute joint constrains the three translational degrees of freedom and two rotational degrees of freedom. Another example of a joint is the translational joint, where two translational degrees of freedom and all three rotational degrees of freedom are removed. When creating a joint two markers will be created. They are called the I- and J-markers. The I-marker belongs to the first part and the J-marker belongs to the second part of the two parts jointed together. For example, the revolute joint between the fork and the wheel, one marker will be on the fork and one marker on the wheel. The two markers will have their z-axis parallel and they will rotate around that axis.

4.4 Forces

A force in ADAMS is a connection between 2 parts that will try to move the parts in a certain way depending on the definition. The movement will be affected by the properties of the parts, i.e. mass, inertia, and other properties of the system.

4.4.1 General force

A general force is a six component force, three forces and three moments, that can be acting on a part. When creating a general force, three markers are created. One marker will be placed on the action part, called the I-marker, one marker on the reaction part, J-marker, and one reference marker. The reference marker can be placed on the ground, which means that the components will be expressed in a system that is not moving with the part. This reference marker could be placed on any part of the model. The reaction part can be the ground and the action part can be any part of the model. Both the I- and J-markers will be placed anywhere on the part but the J-marker belongs to the ground and will not rotate with the I-marker. The I-marker will rotate with the part.

4.5 Adams solver

The kinematic, dynamic and quasi-static analyses in Adams involve the solution of the governing equations of motion. The equations to be solved for the analyses are non-linear algebraic or differential-algebraic equations. It is an iterative process where Adams uses a predictor polynomial to predict the solution to the equations. The order of the predictor polynomial can be as high as twelve. The predictors look at past values and estimates a solution based on them, and the predicted values almost never satisfy the governing equations. An example of a simple first order prediction polynomial can be seen in Figure 13.

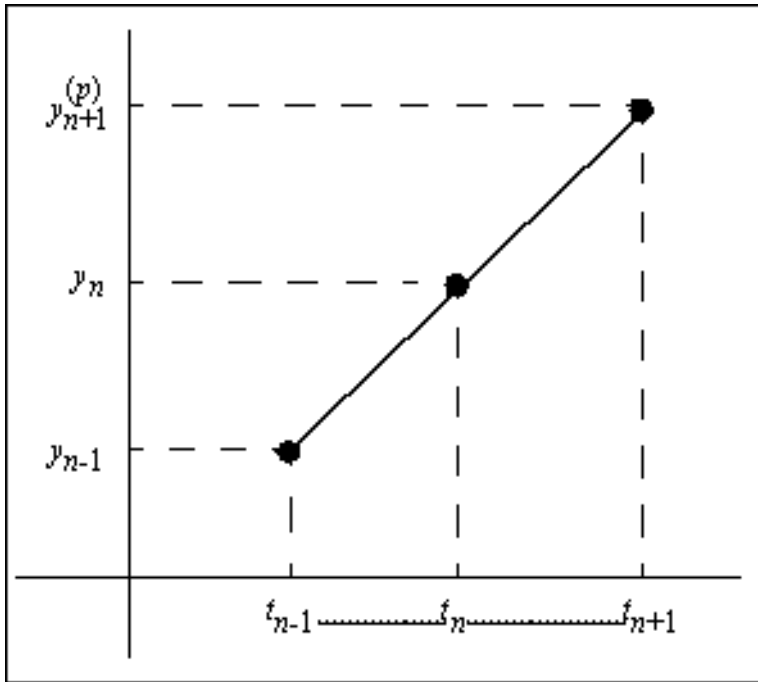


Figure 13 A first order predictor polynomial and the time step made. Online documentation, Adams 2008 r1

If the predicted value is not the solution to the governing equations, an iterative scheme is used to iterate to the solution. A time step is the length of the time step made to the predicted time. If the solution can not be found for the iterations, the size of the time step will be reduced and the iteration process starts again. When the iteration yields a solution to the governing equations the time step is considered to be fulfilled and a new time step can be made and a new predicted solution to the equations can be predicted. An example of a prediction polynomial, corrected values and the time steps made can be seen in Figure 14. The corrected value is the final solution to the governing equations for that specific time step, and it is the value from the iteration process.

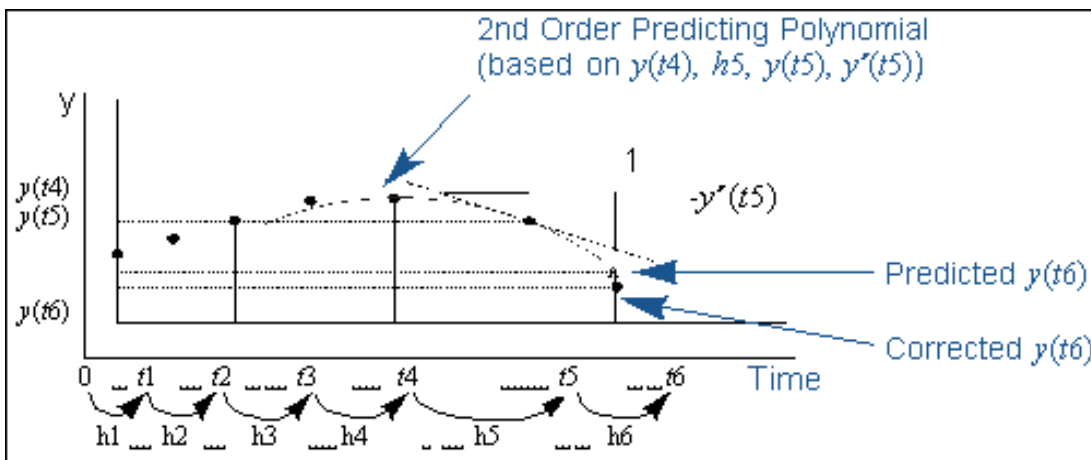


Figure 14 Example of prediction polynomial and time steps. Online documentation, Adams 2008 r1

5 Virtual tunnel face

5.1 Introduction

When the disc cutter has rolled against the rock once some parts of the rock have chipped and some have been crushed and fell away. When the next disc cutter comes, the tunnel face needs to be updated with the new geometry. If the next disc cutter will roll in the track as the first one, then it will roll in the crater created from the first disc cutter. The tunnel face mesh and the reference marker can be seen in Figure 15.

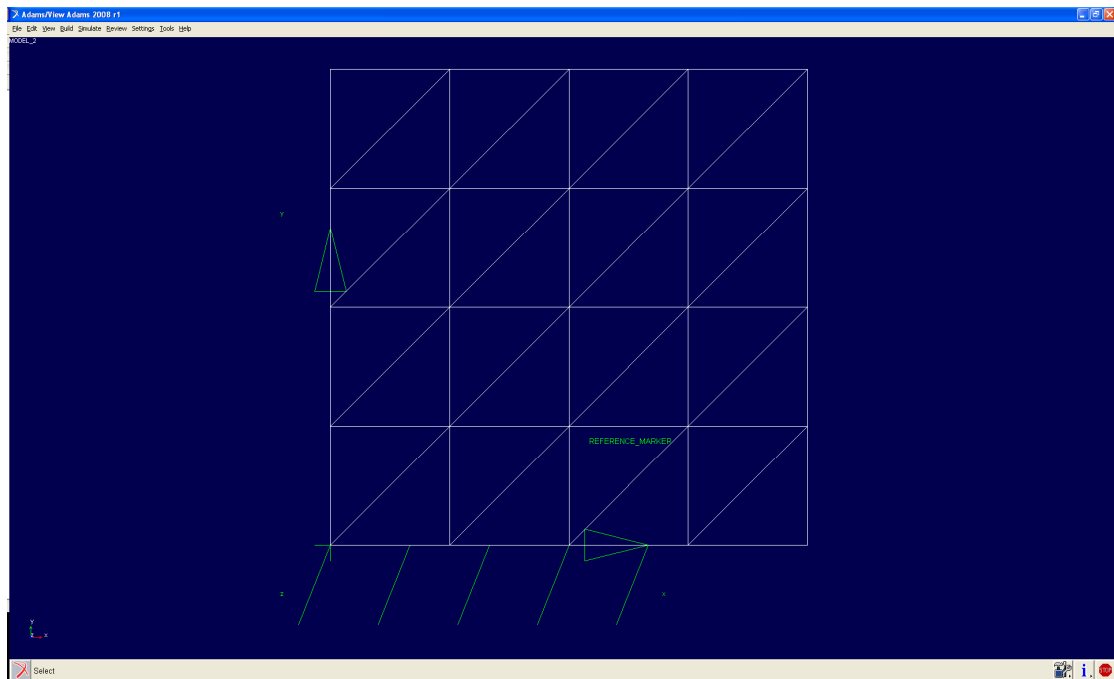


Figure 15 The tunnel face mesh with the reference coordinate system

5.2 Modelling the tunnel face

The tunnel face will be modelled as a large mesh using triangular elements. In each element the surface will be flat. Each node in the mesh corresponds to a height value. The z-coordinates for each node can be changed before starting a simulation. This means that any shape of tunnel face can be studied. The only demand on this model of the tunnel face has is that it must be rectangular. The numbers of nodes in the x- and y-directions do not need to be the same, and the elements do not need to be equilateral. When the first cutter has rolled against the tunnel face the nodal values will be updated with the deformed surface for the next cutter to roll against the new and updated actual geometry of the face. The elements of the tunnel face used in the later simulation work can be seen in Figure 16.

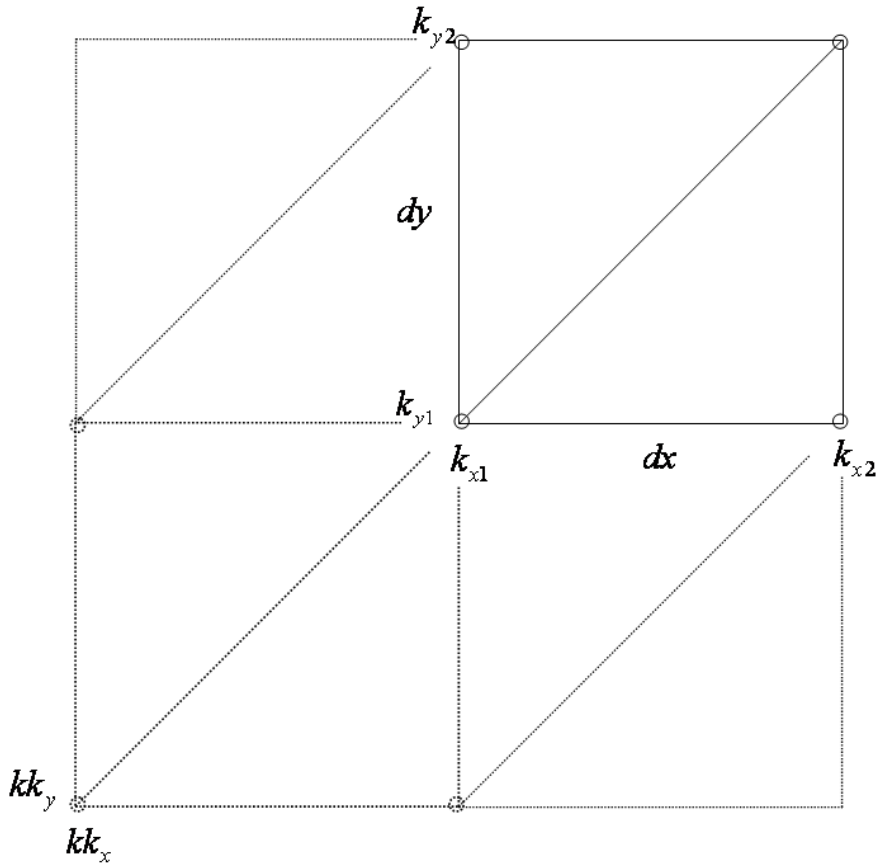


Figure 16 The elements of the tunnel face

In this model of the tunnel face the number of nodes in the x- and y-direction can be chosen, as well as the maximum and minimum values of the coordinates in the x- and y-direction. This means that the tunnel face can be as small and large as the user wishes. When the cutter rolls against the tunnel face, the actual position of the cutter will be measured and by using that position the actual height of the tunnel face can be determined. The height of each node is stored in a matrix, the rock surface matrix, where each row corresponds to the node number in the x-direction and each column corresponds to the node number in the y-direction. For a given position in the mesh the surrounding nodes are calculated according to equations (18) to (23).

$$kk_x = INT\left(\frac{x - x_{\min}}{dx}\right) \quad (18)$$

$$kk_y = INT\left(\frac{y - y_{\min}}{dy}\right) \quad (19)$$

$$k_{x1} = kk_x + 1 \quad (20)$$

$$k_{y1} = kk_y + 1 \quad (21)$$

$$k_{x2} = k_{x1} + 1 \quad (22)$$

$$k_{y2} = k_{y1} + 1 \quad (23)$$

where

$INT(A)$ Rounds A to the nearest integer less than or equal to A

kk_x Start node number in the x-direction

kk_y Start node number in the y-direction

x Actual position of the centre of the disc cutter in the x-direction

y Actual position of the centre of the disc cutter in the y-direction

x_{min} Coordinate of node one in the x-direction

y_{min} Coordinate of node one in the y-direction

dx Element length in the x-direction

dy Element length in the y-direction

k_{x1} Lowest node number in the actual element in the x-direction

k_{y1} Lowest node number in the actual element in the y-direction

k_{x2} Highest node number in the actual element in the x-direction

k_{y2} Highest node number in the actual element in the y-direction

5.3 Elements

For each position in the rock surface matrix, the four surrounding nodes are being calculated. Then the distance between the point of interest and the lowest node number in the x- and y-direction is calculated. The distances between the actual position and the lowest node number in the x- and y-direction are calculated as equations (24) and (25).

$$xx1 = x - (kk_x \cdot dx + x_{min}) \quad (24)$$

$$yy1 = y - (kk_y \cdot dy + y_{min}) \quad (25)$$

These distances are used to determine whether the centre of the disc cutter is in the upper or the lower element of the square rectangle, see Figure 17 and Figure 18. The actual element is determined as:

$$\begin{aligned} \text{if } xx1 < yy1 & \rightarrow \text{upper} \\ \text{else } & \text{lower} \end{aligned} \quad (26)$$

5.3.1 Lower element

The actual position is located in the lower element when the distance between the lowest node number and the actual position in the x-direction is larger than the distance in the y-direction. Otherwise the actual position is located in the upper element. When the location is known and the actual element is determined the derivatives of the heights in the x- and y-directions and the value of the height for that specific position can be calculated according to the equations below, equations (27) to (29).

$$\frac{dz}{dx} = \frac{z(k_{x2}, k_{y1}) - z(k_{x1}, k_{y1})}{dx} \quad (27)$$

$$\frac{dz}{dy} = \frac{z(k_{x2}, k_{y2}) - z(k_{x2}, k_{y1})}{dy} \quad (28)$$

$$z_{rock}(x, y) = z_{rock}(k_{x1}, k_{y1}) + \frac{dz}{dx} xx1 + \frac{dz}{dy} yy1 \quad (29)$$

The case where the actual position is in the lower element can be seen in Figure 17.

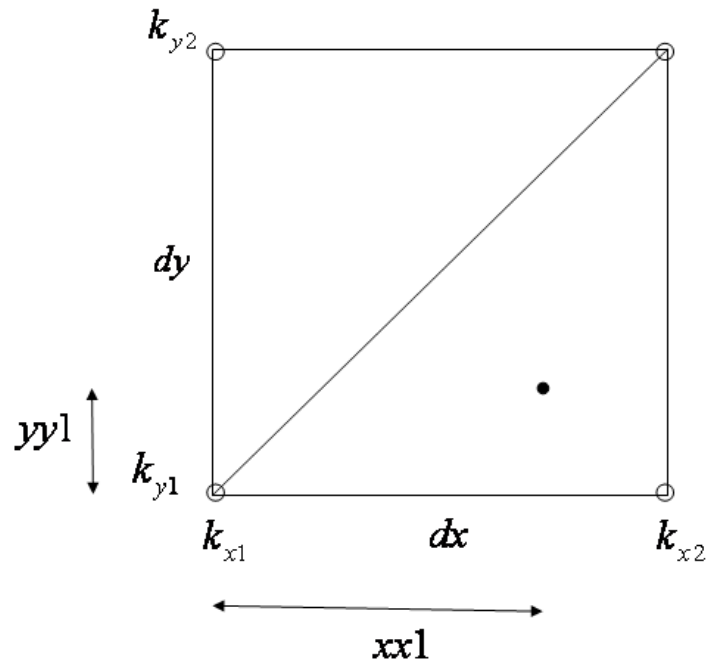


Figure 17 The actual position for a point in the lower element

5.3.2 Upper element

When the actual location is located in the upper element the distance in the x-direction is larger than the distance in the y-direction. The derivatives of the height in the x- and y-direction and the value of the height can now be determined according to the equations below, equations (30) to (32).

$$\frac{dz}{dx} = \frac{z(k_{x2}, k_{y2}) - z(k_{x1}, k_{y2})}{dx} \quad (30)$$

$$\frac{dz}{dy} = \frac{z(k_{x1}, k_{y2}) - z(k_{x1}, k_{y1})}{dy} \quad (31)$$

$$z_{rock}(x, y) = z_{rock}(k_{x1}, k_{y1}) + \frac{dz}{dx} xx1 + \frac{dz}{dy} yy1 \quad (32)$$

The case where the actual position is in the upper element can be seen in Figure 18.

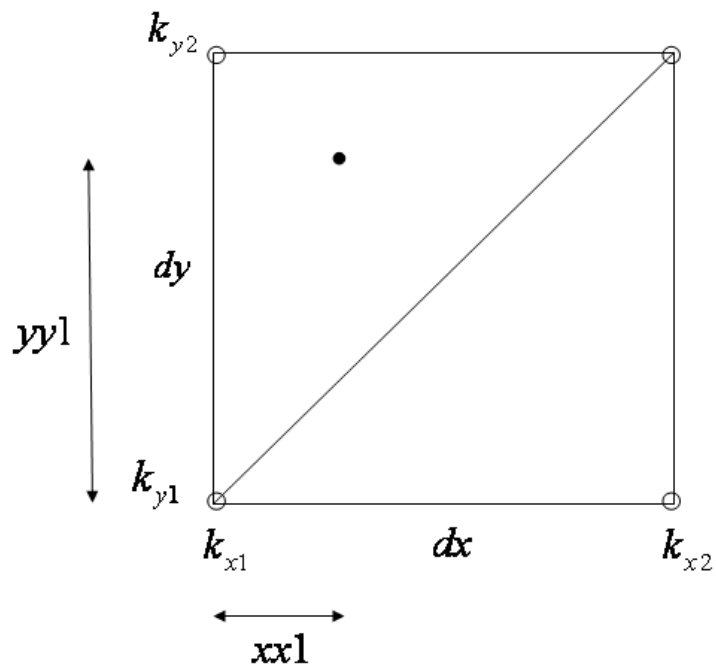


Figure 18 The actual position for a point in the upper element

6 Cutter geometry

The geometry of the disc cutter that is used in the simulation model in Adams can be seen in Figure 19. A common disc diameter is 17 in, and that is the size used in this simulation. The disc radius is an input to each disc cutter used in the simulation model, as well as the small radius r , see Figure 9.

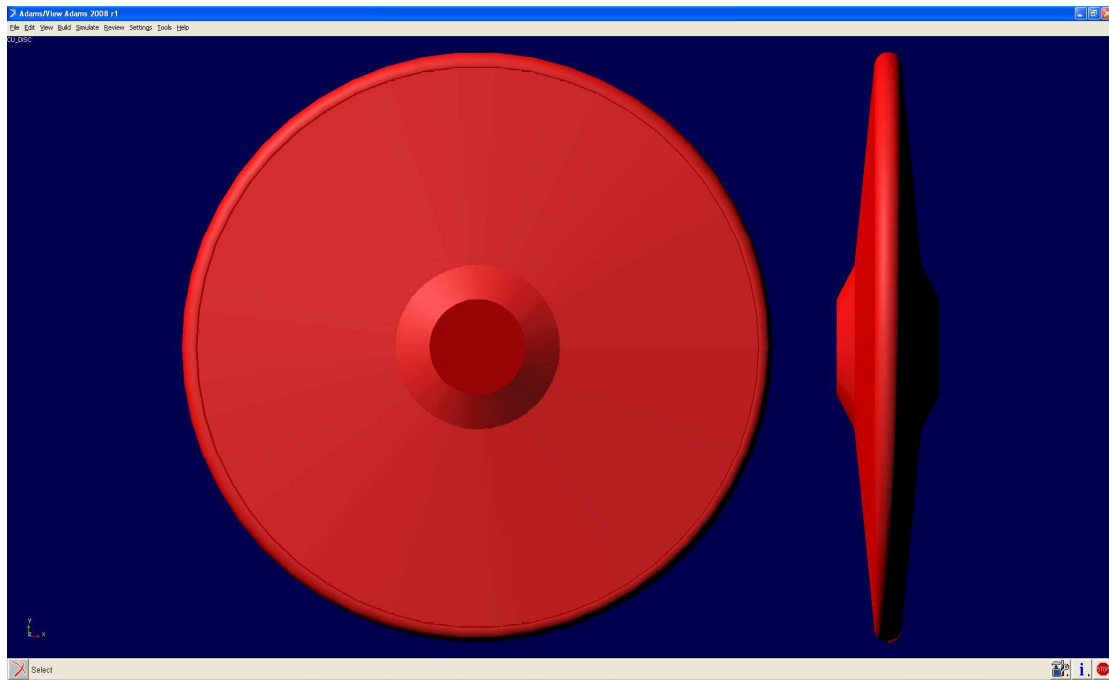


Figure 19 The disc cutter geometry from Adams

6.1 Coordinate systems

Four markers will be used in the computational model, one reference coordinate system on the ground, the reference marker for the general force, common for all cutter discs used in one simulation. One reference coordinate system, marker, on the fork to get the directions of the local coordinate system and to measure the positions and velocities and two joint markers from the joint between the fork and the disc cutter to measure the rotational velocities.

Two coordinate systems will be used in the computational model, the local coordinate system on the disc cutter and the reference coordinate system that the forces and moments will be expressed in. The reference coordinate system will be attached to the ground and the rock surface will be attached to it. The reference coordinate system will therefore not rotate with the disc cutter. The local coordinate system will have its origin at the centre of the disc cutter and will rotate with the fork, but it will not rotate with the disc cutter. The z-axis of the local coordinate system will be parallel to the fork, and the x-axis will be in the direction the cutter is moving. The two coordinate systems can be seen in Figure 20.

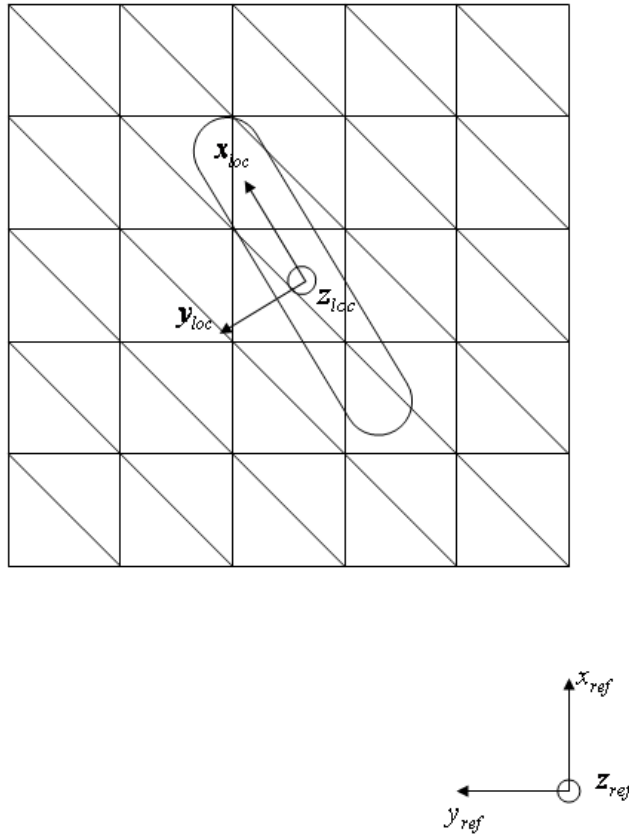


Figure 20 The local and reference coordinate systems

6.2 Coordinate system transformations

In the computation model there are two coordinate systems that are used. The first is the reference coordinate system that is the coordinate system attached to the rock surface and where the forces will be expressed in. The second coordinate system is the local coordinate system. The local coordinate system has its origin in the centre of the disc cutter. In Adams, the yaw-pitch-roll rotation is measured as 3-2-1. The rotation matrices can be seen below, equations (33) to (35). The transformation coordinate systems and angles can be seen in Figure 21.

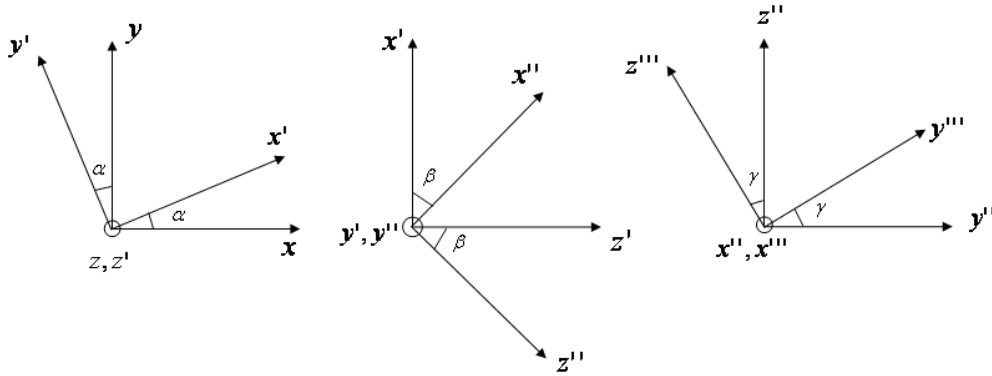


Figure 21 The transformation coordinate systems and the transformation angles

$$R_z(\alpha) = \begin{bmatrix} \cos(\alpha) & -\sin(\alpha) & 0 \\ \sin(\alpha) & \cos(\alpha) & 0 \\ 0 & 0 & 1 \end{bmatrix} \quad (33)$$

$$R_{y'}(\beta) = \begin{bmatrix} \cos(\beta) & 0 & -\sin(\beta) \\ 0 & 1 & 0 \\ \sin(\beta) & 0 & \cos(\beta) \end{bmatrix} \quad (34)$$

Where β is the pitch angle with opposite sign, because Adams measures the rotation sequence 3 -2 1.

$$R_{x''}(\gamma) = \begin{bmatrix} 1 & 0 & 0 \\ 0 & \cos(\gamma) & \sin(\gamma) \\ 0 & -\sin(\gamma) & \cos(\gamma) \end{bmatrix} \quad (35)$$

To go from the reference coordinate system to the local coordinate system one can use the equations below, equations (36) and (37).

$$\begin{bmatrix} x_{local} \\ y_{local} \\ z_{local} \end{bmatrix} = R_{x''}(\gamma)R_{y'}(\beta)R_z(\alpha) \begin{bmatrix} X \\ Y \\ Z \end{bmatrix} = R \begin{bmatrix} X \\ Y \\ Z \end{bmatrix} \quad (36)$$

To go from the local to the global coordinate system the transpose of the transformation matrix is used, see the following equation.

$$\begin{bmatrix} X \\ Y \\ Z \end{bmatrix} = R^T \begin{bmatrix} x_{local} \\ y_{local} \\ z_{local} \end{bmatrix} \quad (37)$$

The rotation angles are measured between the reference coordinate system for the rock surface and a marker in the centre of the wheel, attached to the fork.

6.3 Cutter edge

When searching the edge of the cutter to determine if the cutter has penetrated, a loop will be made over a number of points on the edge of the disc cutter. At first, the coordinates of the centre of the disc cutter are measured. Then the local coordinate system is attached to the centre of the disc cutter with its origin in the centre of the disc cutter and the direction of the coordinate axes from the transformation matrices in Chapter 6.2. At first the local y-coordinate is determined. Then the y-dependent radius is calculated according to equation (38).

$$R(y_{local}) = R - r + \sqrt{r^2 - y_{local}^2} \quad (38)$$

When the y-dependent radius is known the local x- and z-coordinates can be calculated according to equations (39) and (40).

$$x_{local,edge} = R(y_{local}) \cdot \cos(\alpha) \quad (39)$$

$$z_{local,edge} = -R(y_{local}) \cdot \sin(\alpha) \quad (40)$$

The angle α and the local y-coordinate are looped. The angle α is looped from 0 to π radians and the local y-coordinate is looped from $-b$ to b , where b is the width of the disc cutter, see Figure 9. Equations (39) and (40) are explained in Figure 22.

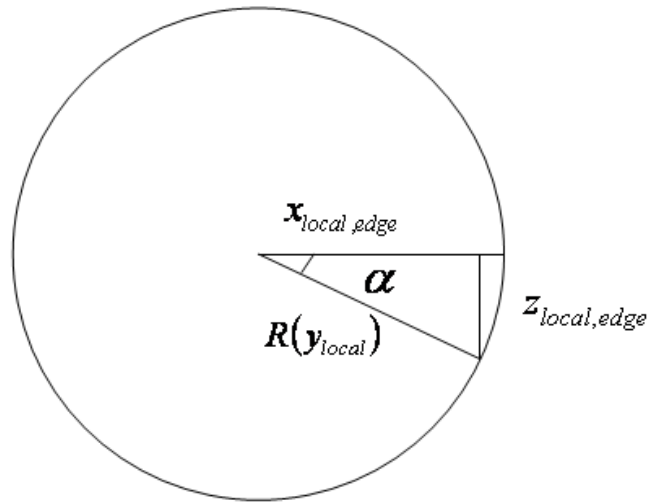


Figure 22 The local x - and z -coordinates on the disc cutter edge

7 Force calculation

7.1 Introduction

The cutter force will act in the direction normal to the surface penetrated by the cutter. In the model presented by Rostami (1997), the cutter force is then divided into a horizontal rolling force and a vertical normal force. The normal force from the model, by Rostami (1997), Figure 11, is normal to the thrust applied. The different forces from the simulation model and their directions can be seen in Figure 23. In Figure 23 the normal force is the normal force to the penetrated plane, the normal force to the penetrated plane is the total force from equation (17), see Figure 11.

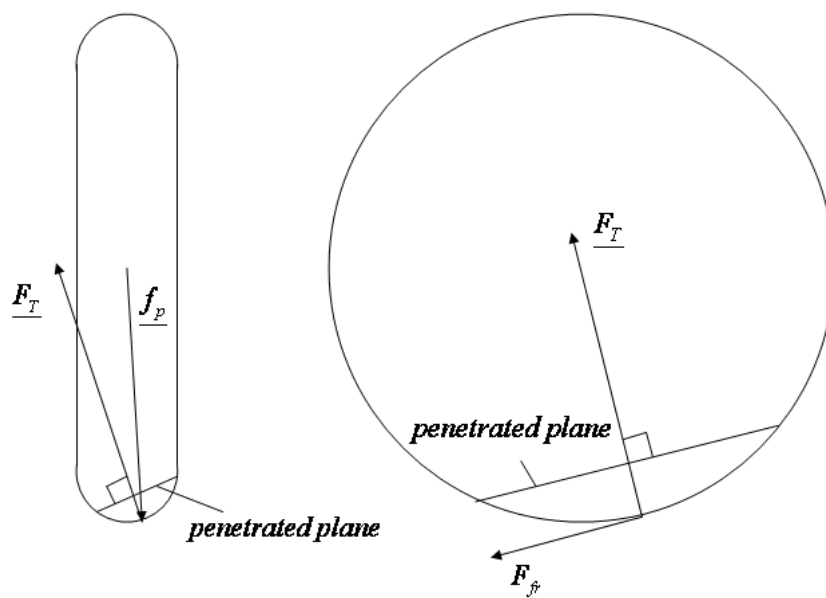


Figure 23 The forces on the disc cutter, cross sectional view to the left and seen from the side to the left

7.2 Force calculations in Adams

The force descriptions found are all calculated locally at the contact point and in the contact plane directions. The force element used, general force, is applied at a marker (I-marker) on the part and this marker is locked during the simulation. The contact between the cutter disc and the mount can occur anywhere on the brim.

The cutter disc is moving with six degrees of freedom. The position of the I-marker can be measured and then the possible contact point (area) can be detected by searching the surface of the brim. If a contact is detected the contact point and plane can be determined and the calculations can be made locally. The local force is then transformed back to the I-marker.

7.3 Penetrated plane

For determination of the direction of the cutting force the penetrated plane needs to be determined. The penetrated area needs to be calculated first. That is done in a subroutine, where a loop is made over the edge of the disc cutter. The edge of the disc cutter is divided into a number of small elements; at first the local y-coordinate is calculated. The local y-coordinate is used to determine the y-dependent radius. The y-dependent radius is then used to calculate the local x-coordinate and the local z-coordinate. When the local coordinates are known they are transformed into the global coordinate system as described in Chapter 6.2. For every point in the z-coordinate of the rock surface is calculated as described in Chapter 8.1. If the wheel has penetrated into the rock surface, i.e. the z-coordinate of the wheel is smaller than the z-coordinate of the mesh, the three coordinates for the mesh element are stored in three vectors.

7.4 Normal vector

When the loop in the previous section has reached a point on the wheel that has penetrated into the rock surface another subroutine is called. This subroutine makes a search in the mesh and calculates the four surrounding nodes and determines in which element the point is. Then it calculates the two vectors on the edges of the element and calculates the cross product between them which gives the normal to the element. The normal is calculated using equation (41) and (42).

For the upper element, Figure 24:

$$\underline{e}_n = \underline{v}_1 \times \underline{v}_2 \tag{41}$$

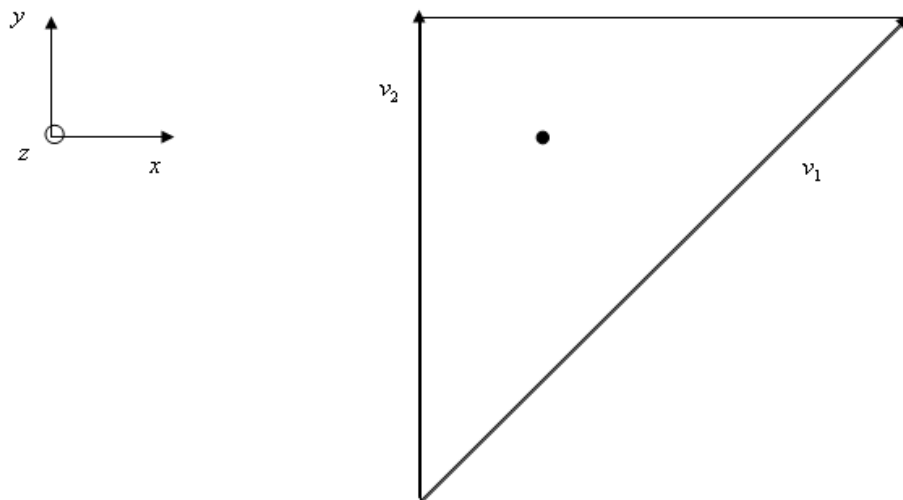


Figure 24 Vectors for calculating the element normal in the upper element.

For the lower element, Figure 25:

$$\underline{e}_n = \underline{v}_1 \times \underline{v}_2 \quad (42)$$

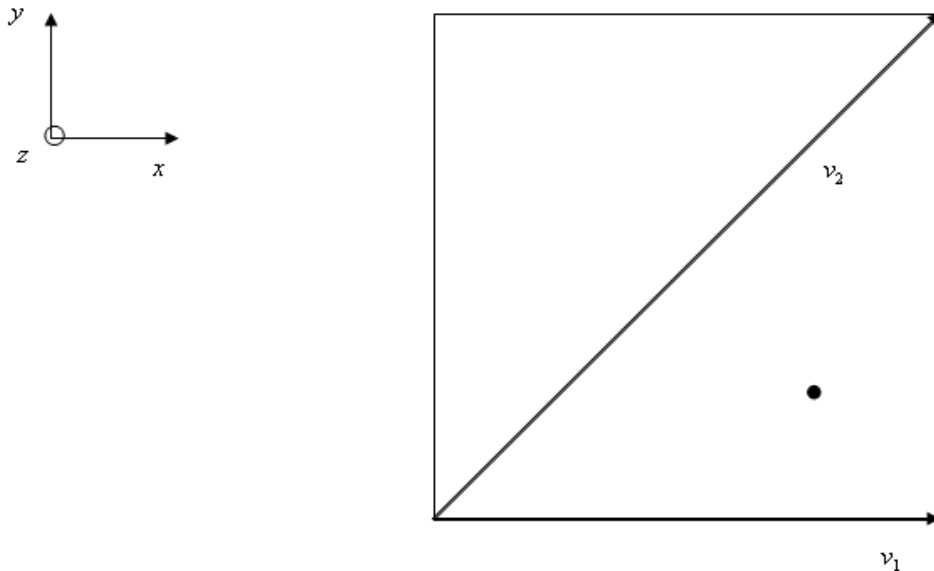


Figure 25 Vectors for calculating the normal in the lower element.

The normal vector is normalized and stored. All the normal vectors calculated in the loop are stored and all the unique normal vectors are summed. The summation of the normal vectors is then normalized. By doing that a mean normal vector has been calculated for the penetrated plane. This vector is the normal vector to the penetrated plane and is called \underline{N} .

When all the points on the disc cutter have been looped over, a vector is calculated between the first point and the last point stored, vector one. After that the cross product between the normal vector and the vector calculated between the first and the last point is calculated, vector two. The plane defined by vector one and vector two is called the penetrated plane.

The centre of the penetrated plane is in the middle of vector one and is calculated as:

$$\underline{p}_c = \underline{p}_1 + 0.5 \cdot \underline{s}_1 \quad (43)$$

The forces will be applied onto the edge of the disc cutter on the point at the edge of the wheel where the vector from the centre of the wheel to the centre of the plane crosses the cutter edge, see Figure 26. The vector from the centre of the disc cutter to the point of force application is called f_p .

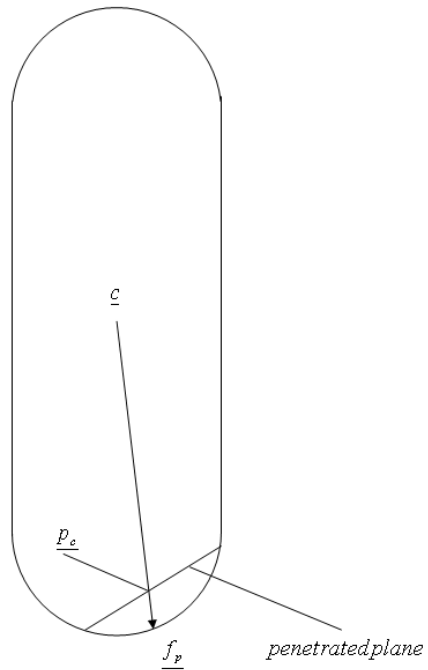


Figure 26 A cross sectional view of the penetrated plane and a definition of the point of force application

The penetrated plane viewed from above can be seen in Figure 27. The figure also shows the direction vectors of the penetrated plane and the normal to the penetrated plane.

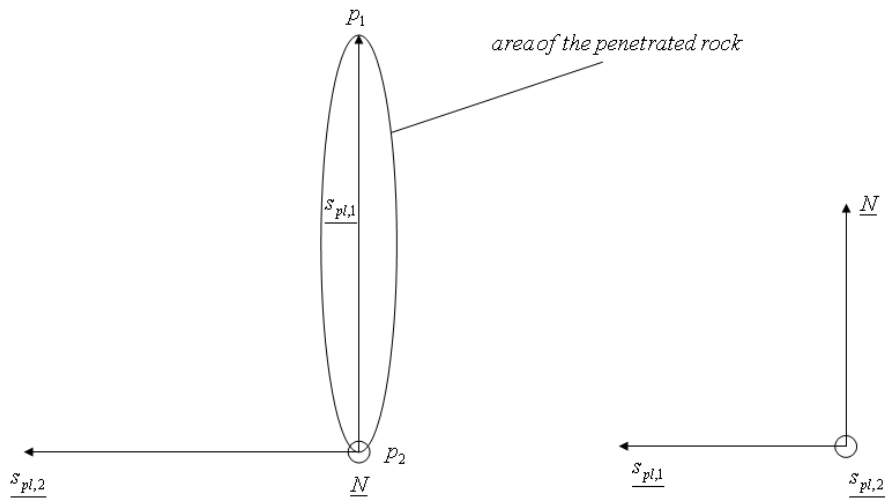


Figure 27 The two vectors defining the penetrated plane and the normal to the penetrated plane for the ideal case with a flat and horizontal tunnel face

All the lengths and angles for the following calculations, equations (44) to (53), can be seen in Figure 28. When the centre of the penetrated plane is calculated the direction of the \underline{f}_p vector can be calculated. That vector is calculated according to equation (44).

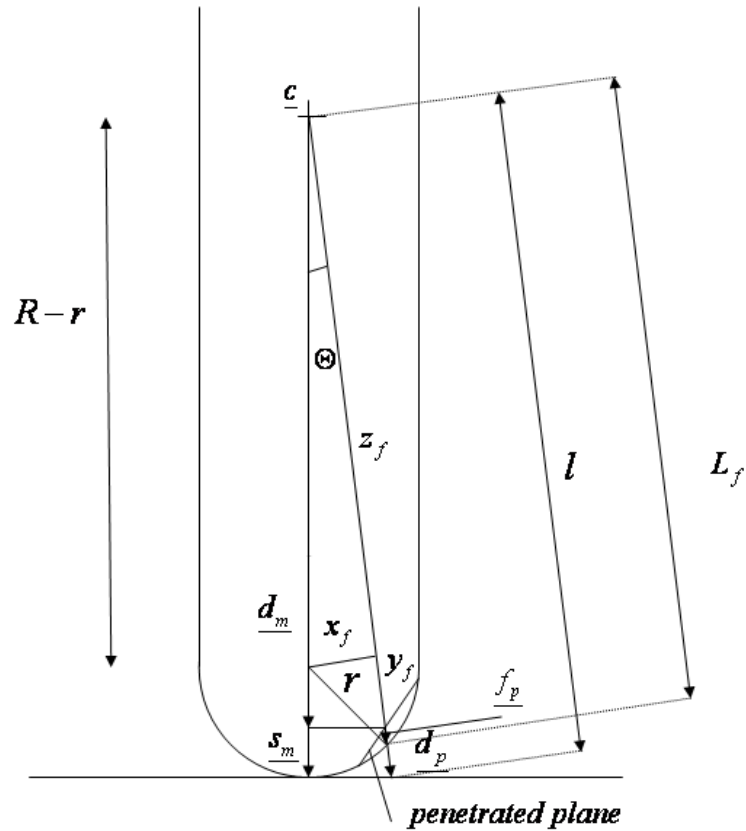


Figure 28 The lengths and vectors for calculating the point of force application

$$\underline{d}_p = \underline{p}_c - \underline{c} \quad (44)$$

The direction vector will then be transformed into the local coordinate system using the transformation matrices in Chapter 6.2. When the local coordinates are known for the direction vector, the vector from the centre of the disc cutter to the point in the edge of the disc cutter with the same local z-coordinate as the p_c but with the local y-coordinate in the centre of the disc cutter, zero, can be calculated. That vector is calculated according to equation (45).

$$\underline{d}_m = \underline{d}_p(1) \cdot [1 \ 0 \ 0] + \underline{d}_p(3) \cdot [0 \ 0 \ 1] \quad (45)$$

That vector will then be multiplied with the disc cutter radius, according to equation (46), which will give a vector from the centre of the disc cutter to the brim of the disc cutter.

$$\underline{s}_m = R \cdot \begin{pmatrix} \underline{d}_m \\ |\underline{d}_m| \end{pmatrix} \quad (46)$$

Then the length to the point in the direction of the \underline{d}_p vector from the centre of the wheel to the point with the same local z-coordinate as the \underline{s}_m point, see Figure 28, can be calculated, according to equation (47).

$$l = \frac{R \cdot \text{length}(\underline{d}_p)}{\text{length}(\underline{d}_m)} \quad (47)$$

Then the angle between the \underline{s}_m vector and the \underline{d}_p vector can be calculated according to equation (48).

$$\Theta = \cos^{-1}\left(\frac{R}{l}\right) \quad (48)$$

Then the x_f length can be calculated according to equation (49).

$$x_f = \sin(\Theta) \cdot (R - r) \quad (49)$$

And the y_f can be calculated according to equation (50).

$$y_f = \sqrt{r^2 - x_f^2} \quad (50)$$

When the y_f is calculated the z_f can be calculated according to equation (51).

$$z_f = \cos(\Theta) \cdot (R - r) \quad (51)$$

When all the lengths are known the length of the vector from the centre of the disc cutter to the point on the edge where the forces will be applied can be calculated according to equation (52).

$$L_f = y_f + z_f \quad (52)$$

The \underline{f}_p vector can finally be calculated according to equation (53).

$$\underline{f}_p = L_f \cdot \underline{d}_p \quad (53)$$

7.5 Penetration

The penetration is one of the factors determining the size of the force that will act on the disc cutter. When the penetrated plane is calculated one can calculate the penetration depth. The penetration depth is calculated as the difference in the local z-coordinate of the penetrated point with the highest local z-coordinate and the penetrated point with the lowest local z-coordinate. The penetration depth is calculated according to equation (54).

$$\text{penetration} = |z_{l,p1} - z_{l,p2}| \quad (54)$$

7.6 Friction

There will be a friction force acting on the disc cutter at the point on the edge of the disc cutter where the forces will be applied. The friction force will be calculated as the normal force, normal to the penetrated plane, multiplied by the friction coefficient. The equation for the friction force is:

$$F_{fr} = -F_N \cdot \mu \quad (55)$$

To be able to calculate the friction coefficient the velocity of the disc cutter edge relative the penetrated plane needs to be determined. The friction coefficient as a function of the velocity can be seen in Figure 29, and is thoroughly described in Appendix A, Chapter A.2.2.

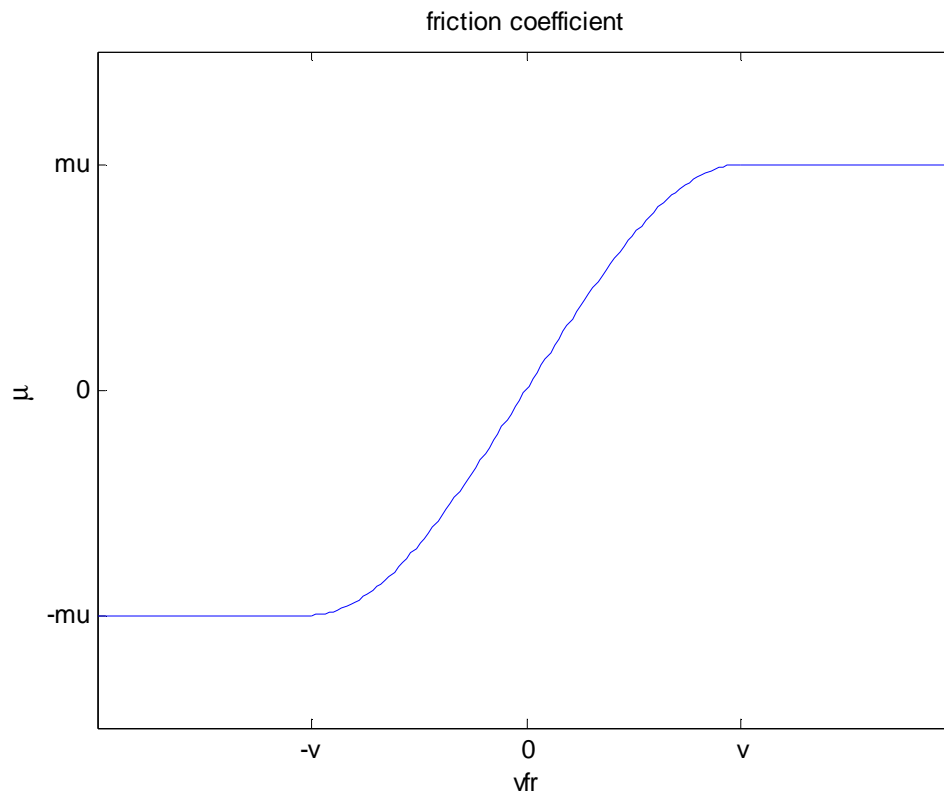


Figure 29 The friction coefficient as a function of the velocity

7.6.1 Velocity

The penetrated plane is used to calculate the velocity for the friction. The translational velocities of the centre of the disc cutter are measured using the Adams built in function TVEL which generates all three translational velocities expressed in the reference coordinate system. The three rotational velocities of the disc cutter are measured using the Adams built in functions WX, WY and WZ. They give the rotational velocities of the disc cutter expressed in the local coordinate system. The rotational velocities of the disc cutter are transformed from the local coordinate

system into the reference coordinate system using the transformation matrices presented in Chapter 6.2. The vector from the centre of the disc cutter to the point of the disc cutter where the force will be applied is used to calculate the velocity in that point. This is done according to

$$\underline{VREF} = \underline{TVEL} + \underline{\omega} \times \underline{r} \quad (56)$$

When the velocity of that point on the disc cutter is known the velocity needs to be transformed to the penetrated plane. The transformation is done using equation (57) and the transformation vectors can be seen in Figure 27.

$$\underline{v}_{pl} = \begin{bmatrix} s_{pl,1} \\ s_{pl,2} \\ e_n \end{bmatrix} \underline{VREF} \quad (57)$$

This transformation gives the velocity in the three directions, the first two values are the velocities in the directions of the direction vectors of the plane and the third component is the velocity in the direction of the normal vector. The magnitude of the velocity in the plane is calculated as the square root of the sum of the first two components of the velocity vector from the plane according to equation (58).

$$v_{fr} = \sqrt{v_{pl}(1)^2 + v_{pl}(2)^2} \quad (58)$$

The two velocity vectors for the penetrated plane and the sum of them, the friction velocity, can be seen in Figure 30.

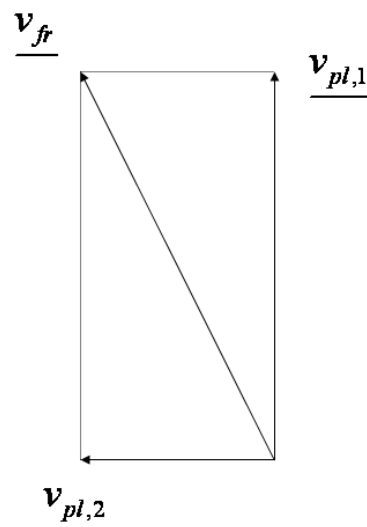


Figure 30 The two velocity vectors in the penetrated plane and the friction velocity

The direction of the friction force is opposite to the friction velocity. The first two components of the plane velocity vector is the velocity in the direction of the sum of the two vectors defining the plane. The direction of the friction velocity is calculated by adding the two velocity vectors of the penetrated plane, which can be seen in equation (59).

$$\underline{v}_{fr} = \underline{v}_{pl}(1) \cdot \underline{s}_{pl,1} + \underline{v}_{pl}(2) \cdot \underline{s}_{pl,2} \quad (59)$$

The equation above defines the direction of the friction force, and since there is a minus sign in the equation for the friction force the friction force vector can be calculated as

$$\underline{F}_{fr} = F_{fr} \cdot \left(\frac{\underline{v}_{fr}}{|\underline{v}_{fr}|} \right) \quad (60)$$

7.6.2 Friction coefficient

When the friction velocity is known the friction coefficient can be calculated. The friction coefficient is a function of the friction velocity and is determined from Figure 29.

7.7 Cutter force

When the normal vector is calculated the direction of the cutter force can be calculated. The cutter force is the force calculated from the force model presented in Chapter 3.3, and can be seen in Figure 11. Since the cutter force always will work in the direction of the normal vector from the penetrated plane the components of the cutter force can be calculated using equation (61) to (65).

$$F_x = n_x F_T \quad (61)$$

$$F_y = n_y F_T \quad (62)$$

$$F_z = n_z F_T \quad (63)$$

The three equations for the components of the cutter forces can be written in the following way

$$\underline{F}_T = \underline{N} F_T \quad (64)$$

The total force that will be acting on the disc cutter in the point of force application is the addition of the cutter force vector and the friction force vector. The total force is calculated according to

$$\underline{F}_{tot} = \underline{F}_T + \underline{F}_{fr} \quad (65)$$

This is possible to do since all the components of the forces are expressed in the reference coordinate system.

7.8 Cutter moment

The cutter force calculated in the section above will be translated to the centre of the disc cutter to the general force. Since the general force is applied in the centre of the disc cutter and the forces are working on the edge of the disc cutter a moment needs to be attached to the general force.

The moment of the cutter force about the centre of the disc cutter is calculated according to equation (66) where \underline{f}_p is given by equation (53).

$$\underline{M}_{tot} = \underline{f}_p \times \underline{F}_{tot} \quad (66)$$

The total force vector and the distance vector have their components expressed in the reference coordinate system. The moment will be the moment around the three axes of the reference coordinate system.

8 Rock fragmentation

8.1 Deformation

When the cutter rolls against the rock a crushed zone will appear. The shape of the crushed zone is presented more thoroughly in Chapter 2.3, but is assumed to be ellipsoidal, with the smallest radius in the direction of the cut and the largest radius parallel to the cut.

The update of the rock surface matrix will be made in the subroutine DEFORM. A loop will be made over all the nodes in the entire mesh. The coordinates of each node will be calculated using equation (67) to (69).

$$x_{coord} = rockx_{min} + rockdx(L-1) \quad (67)$$

$$y_{coord} = rocky_{min} + rockdy(K-1) \quad (68)$$

$$z_{coord} = rockz(L, K) \quad (69)$$

Then a vector will be calculated from the centre of the disc cutter to the node of interest, according to the following equation.

$$\begin{bmatrix} x \\ y \\ z \end{bmatrix} = \begin{bmatrix} x_{coord} \\ y_{coord} \\ z_{coord} \end{bmatrix} - \begin{bmatrix} x_{centre} \\ y_{centre} \\ z_{centre} \end{bmatrix} \quad (70)$$

The coordinates of the vector from the centre of the disc cutter to the node of interest will be transformed into the local coordinate system described in Chapter 6.1. If the local y-coordinate is less than half the width of the disc cutter and the local x-coordinate is smaller than the large radius of the disc cutter the y-dependent radius can be calculated as in Chapter 6.3. The nodes are within the area shadowed by the disc cutter if the local x-coordinate is less than the y-dependent radius. Then the z-value of the node can be calculated and compared to the z-value on the point on the wheel with the same local x- and y-coordinates. The area shadowed by the disc cutter can be seen in the figure below. If the node is inside the shadowed area it might be penetrated by the disc cutter, otherwise not.

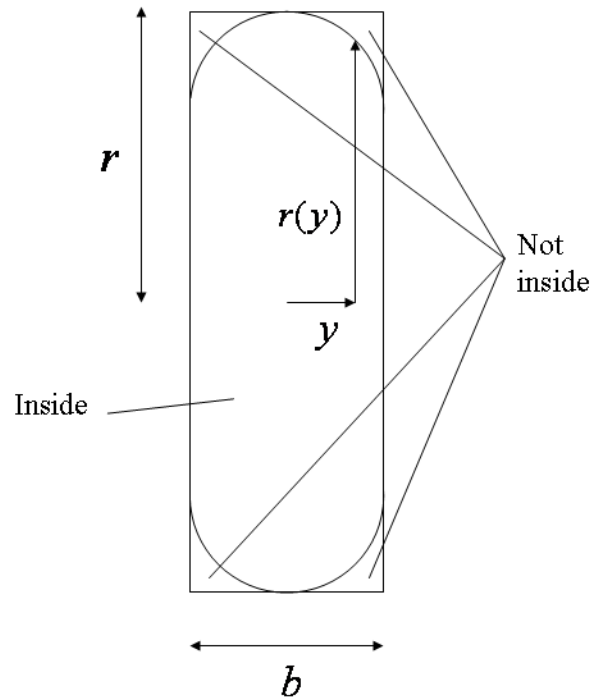


Figure 31 Figure over the shadowed area.

When the disc cutter is within the shadowed area, see Figure 31, it might penetrate into the rock. The z -coordinate of the node is calculated above in equation (69) and will be compared to the z -coordinate of the wheel for the corresponding x - and y -coordinate. The local y -coordinate of the wheel is used to calculate the y -dependent radius as above. When the radius is known the z -coordinate can be calculated using equation (71).

$$z_{disc} = \sqrt{r(y_{coord})^2 - x_{coord}^2} \quad (71)$$

The z -coordinate of the disc is then compared to the z -coordinate of the node. If the z -coordinate on the disc cutter is lower than the one on the node the disc has penetrated into the rock surface.

8.2 Matrix update

If the point on the wheel surface has penetrated into the rock surface and created an inelastic deformation the rock surface matrix must be updated with a new z -value for that specific node. In this case all of the penetration into the rock surface has been seen as an inelastic deformation.

In this model the rock fragmentation is simplified. When the time step is achieved, the temporary rock matrix will be copied to the rock matrix. The penetration into the rock

will be reduced from the node that is penetrated in the rock surface matrix. The updating is done according to equation (72).

$$trockz(L, K) = rockz(L, K) - (rockz(L, K) - z_{disc}) \quad (72)$$

8.2.1 Temporary rock matrix

When there is an inelastic penetration into the rock surface causing a deformation of the rock a temporary rock matrix is created. From the temporary rock matrix a certain part of the z-value of the node of interest is removed, in this case all of the penetration depth. If the time step is successful the temporary rock matrix is copied to the rock matrix, but if the time step is not successful the temporary rock matrix will not be copied. If the time step is too long and the system can not be solved the length of the time step needs to be shortened. When this happens the temporary matrix will be replaced with the rock matrix since the temporary rock matrix is not valid when the time step is decreased and the simulation time decreases.

9 Model validation

The model will be validated by simulating rock cutting with a disc cutter on a flat rock surface. The resultant forces will be compared to a similar case from the literature, so the model can in some sense be validated.

9.1 Inputs

The inputs to Adams will be given as in Appendix A. For each cutter a specific force number can be given, large and small radius for the cutter, see Figure 32. As described in Appendix A.2.3, the special ID-series are given, they contain the markers that will be used for each cutter to calculate the position, velocity, rotational velocity and rotational angles. The different markers used can be seen in the figure below. All the parameters that can vary, and do not need to be equal for all cutters in a simulation, are sent to the subroutine in the general force.

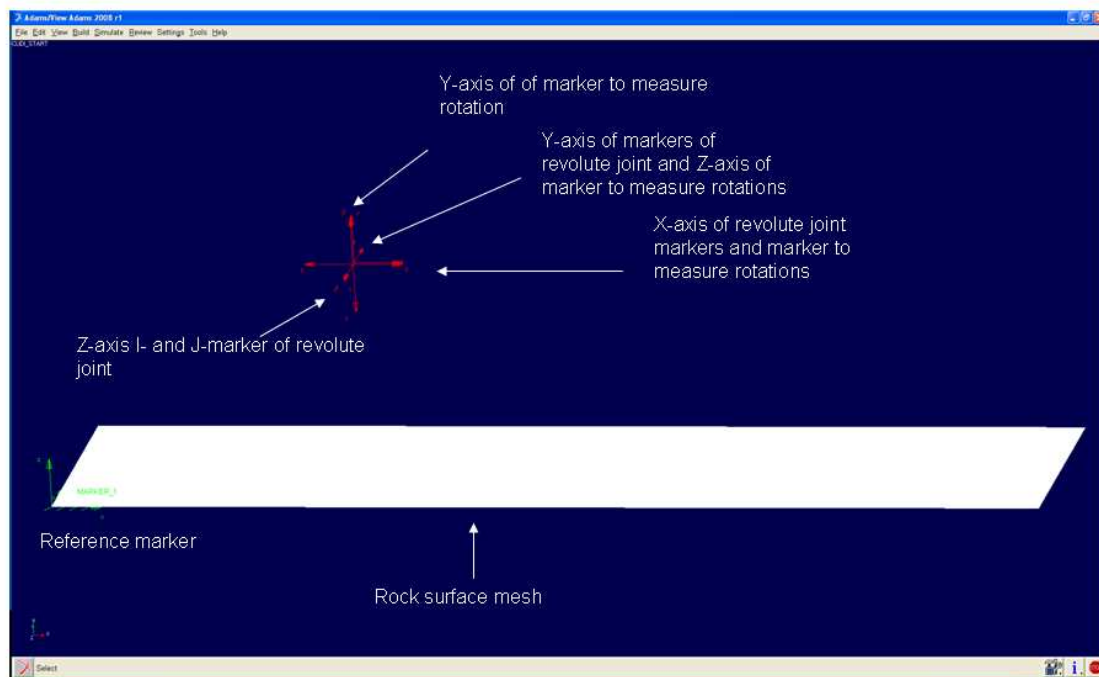


Figure 32 The markers used in the simulation and the corresponding directions

Inputs that are valid for all the parts in the simulation as the friction values, the compressive and tensile strength of the rock are stored in a common vector and used in the simulation. These values are the same for all the disc cutters in one simulation.

In this specific model validation the forces from the simulation model will be compared to an LCM test from the literature. The input values and the results are from Gertsch et al (2007) and can be seen in Table 2. The disc cutter will have a large radius of 17 in and a small radius of 0.5 in. The cutting speed will be 1.0 m/s and the length of the cut will be 1 m. Only one disc cutter will be used but to be able to compare to the case from the literature a spacing of 51 mm will be used. The compressive strength of the rock in this test is 158 MPa, and the tensile strength of the

rock will be 6.78 MPa. The tip width of the disc cutter is 13 mm. The penetration will be set to 3.8 mm.

Table 2 The input values for the simulation test

R [mm]	C	Uniaxial compressive strength [MPa]	Brazilian tensile strength [MPa]	Spacing [mm]	Cutting speed [m/s]	Penetration [mm]
215.9	2.12	158	6.78	51	1	3.8

9.2 Theoretical force

The theoretical force for the given rock parameters, penetration depth and spacing as given above is calculated according to equation (72).

$$F_T = TR\phi P' \quad (72)$$

With the given numbers from above, the mean value of the force on the disc cutter will be, according to the equation (74), 61.1 kN. The mean pressure in the pressure zone, see Figure 11, is calculated according to equation (73).

$$P' = C\sqrt[3]{\frac{\sigma_c^2 \sigma_t S}{\sqrt{RT}}} = 2.12 \cdot \sqrt[3]{\frac{(158 \cdot 10^6)^2 \cdot 6.78 \cdot 10^6 \cdot 0.051}{\sqrt{0.2159 \cdot 0.013}}} = 115.8 \text{ MPa} \quad (73)$$

The pressure calculated in equation (73) is used in equation (74) to calculate the total force.

$$F_T = TR\phi P' = 0.015 \cdot 0.2159 \cdot \cos^{-1}\left(\frac{0.2159 - 0.0038}{0.2159}\right) \cdot 115.8 = 61.1 \text{ kN} \quad (74)$$

From equation (15) and (18), the rolling and normal forces can be calculated, according to equation (75) and (76).

$$F_N = TR\phi P' \cos\left(\frac{\phi}{2}\right) = F_T \cdot \cos\left(\frac{\phi}{2}\right) = 61.1 \cdot 10^3 \cdot \left(\frac{0.2159 - 0.0038}{0.2159}\right) = 60.8 \text{ kN} \quad (75)$$

$$F_R = F_N \cdot \tan\left(\frac{\phi}{2}\right) = 61.1 \cdot 10^3 \cdot \tan\left(\cos^{-1}\left(\frac{0.2159 - 0.0038}{0.2159}\right)\right) = 5.8 \text{ kN} \quad (76)$$

9.3 Simulation force

A simulation will be made with the inputs given in Table 2. The model before the simulation starts can be seen in Figure 33.

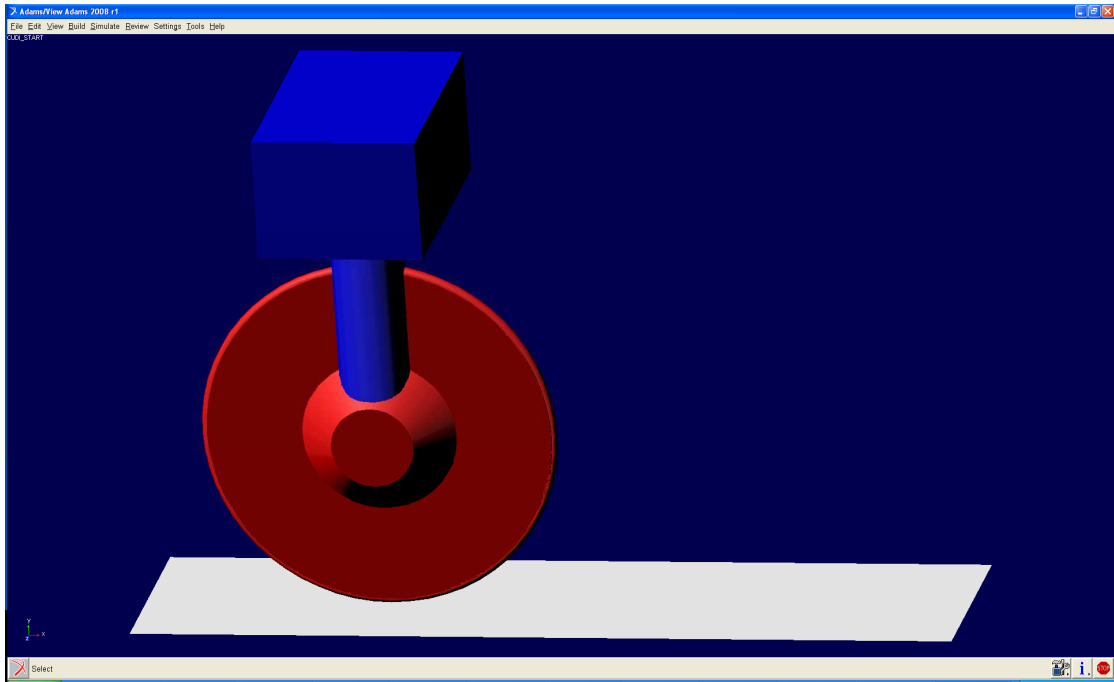


Figure 33 The simulation model before starting the simulation

The forces from the general force can be seen in Figure 34, Figure 35 and Figure 36.

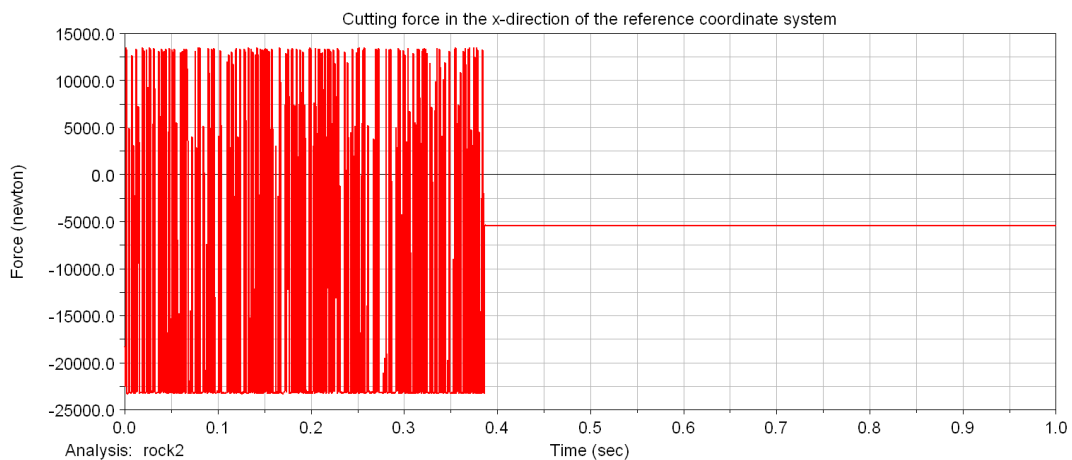


Figure 34 The cutting force in the x-direction of the reference marker

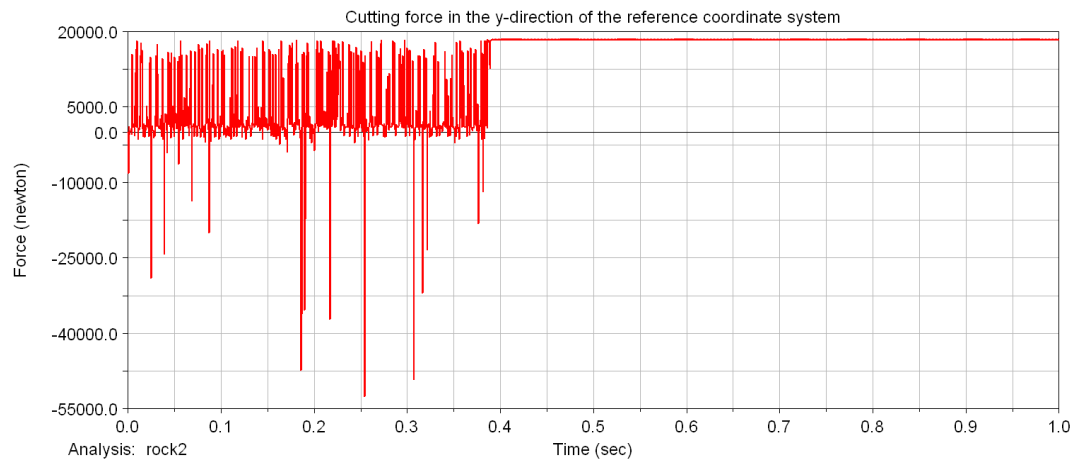


Figure 35 The cutting force in the y-direction of the reference marker

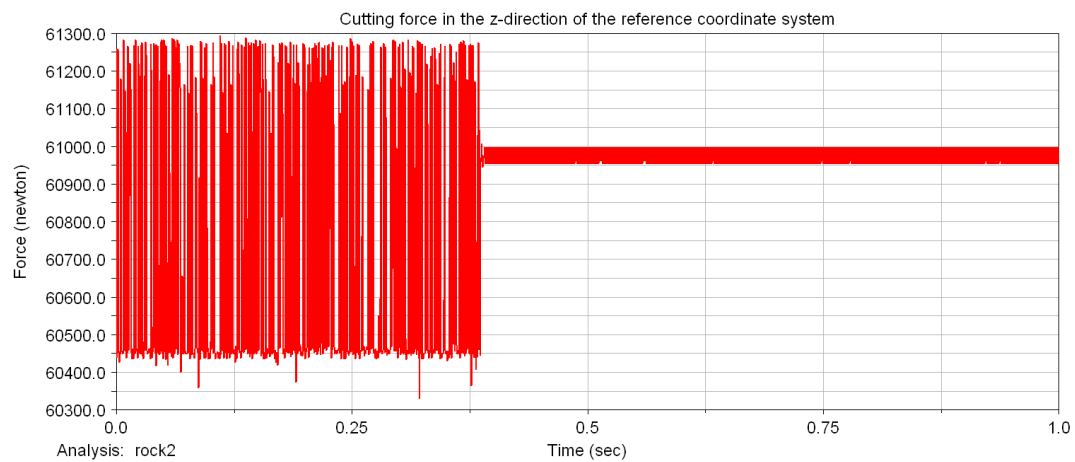


Figure 36 The cutting force in the z-direction of the reference marker

During the simulation, one can choose when the rock surface matrix will be saved. For instance, if a simulation needs to be continued at a certain time, the old rock surface matrix saved from an older simulation can be used as the start rock surface matrix. To view the rock surface matrix in Adams the file type .shl is used. One can save the .shl file on the same way as the rock surface matrix. The .shl is the shell file type where the nodes and how they are linked are stored. In the subroutine for the force calculations the file type .rsf is used. In the .rsf file, rock surface file, the node numbers and their coordinates are stored. The rock surface matrix is attached to the reference marker and has its directions in the reference coordinate system.

The shape of the updated and deformed rock surface mesh after the simulation can be seen in Figure 37.

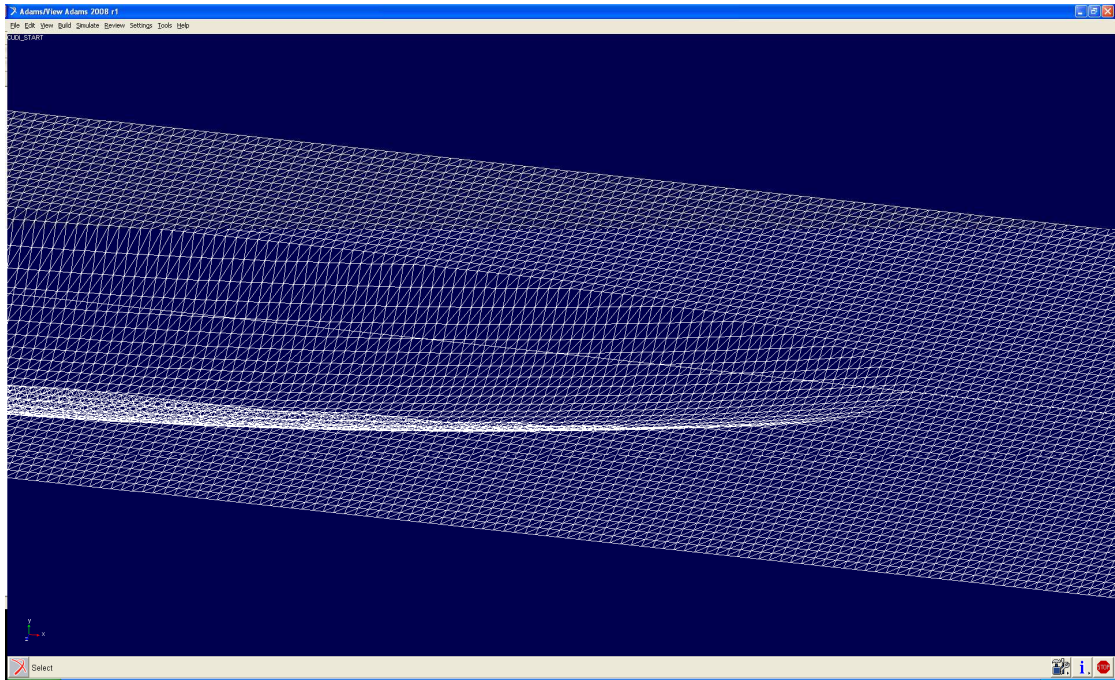


Figure 37 The updated rock surface, note the triangular elements and the deformation



Figure 38 The rock surface attached to the reference marker

9.4 Comparison

The forces from the real test in a LCM compared to the results from the theoretical formula and the simulation can be seen in Table 3.

Table 3 Table over the forces from the theoretical force model, a real test in a LCM and from an Adams simulation with the model developed in this Master Thesis

Model	Spacing [mm]	Penetration [mm]	Average cutter force (normal) [kN]	Average cutter force (rolling) [kN]	Average cutting force (side) [kN]
Theoretical	51	3.8	60.8	5.8	-
Test in LCM	51	3.8	81	7.3	11.2
Simulation	51	3.8	60.9	13.4	12.6

Table 3 shows that the average cutter normal force is higher in the LCM test than in the simulation and the theoretical calculation. The simulation and the theoretical calculation give almost the same value for the average normal force. The average rolling force for the theoretical calculation and the LCM test is close each other while the simulation generates a higher rolling force. The side force from the simulation and the LCM test is almost the same.

10 Model limitations

10.1 Detecting penetration

The loop made over the surface of the disc cutter to detect if it has penetrated or not is only made on the double curved surface of the disc cutter. If the side of the disc cutter is touching the rock it will not be detected. The loop is only made for negative z-coordinates of the local coordinate system, which means that if the double curved area of the disc cutter is in contact with the mount on a positive local z-coordinate the contact will not be registered for that point. This should not influence the reliability of the simulation model.

10.2 Penetrated plane

The penetrated plane is assumed to be a flat plane, this is an assumption and a simplification made. This is not completely true but it will not influence the result so much. The direction of the cutter is correctly calculated since it is the mean normal of all the points penetrated by the disc cutter.

10.3 Chipping

This simulation model does not take the side chipping or the cracking process into consideration at this stage. To be able to use this model to simulate a complete tunnelling operation the chipping and cracking process needs to be taken into account. Since the chipping is not studied, the behaviour of the forces and moments of this model is not completely true since the dynamic behaviour of the force is not studied. As mentioned in Chapter 2.3.4, the magnitude of the cutting force will decrease when a chip is created and after that increase again until the next chip is created. The variation in force can not be studied but the size of the forces and moments and their directions can be studied using this simulation model.

11 Discussion and results

As can be seen in Table 3, the forces from the simulation and from the theoretical formula are almost equal. This is because that the penetration in the model is set to the same value as the penetration in the theoretical formula. The reason for the larger rolling force in the simulation model is that the friction force is working in the beginning of the simulation, see the first 0.4 s of simulation in Figure 34. From Chapter 3.2.2 one can see that the cutter force is working in the loading zone. In the simulation model the cutter force is assumed to work in the centre of the penetrated plane, see equation (43), Figure 23 and Figure 26. The point of force application can easily be changed in equation (43) and the constant C in equation (15) can be optimized for the specific rock and cutting condition to be studied.

To make a simulation on a flat ground like this is a good way of calibrating the computational model. For instance, the constant value of C in equation (15) can be adjusted so that the forces are matching the forces obtained from measurements on a test rig or a linear cutting machine (LCM). Other parameters to adjust are the friction coefficient for example.

A calibrated model can be used for simulations of the forces acting on the disc cutter while cutting rock for any geometry of the rock surface. The simulation model can also be used to link a number of cutters together to create a tunnel boring machine for instance, to study the total force acting on the drum of the machine. The total force can then be used to design the front parts of the machine to withstand it and to design an automatic control system.

The simulation model is built such that many disc cutters can be linked together to a real tunnel boring machine. Because of that the usage of the model increases. The force model can be updated, a number of simulations can be done and the results from them can be used to update the force model. For a given set of parameters, such as penetration, spacing, compressive strength etc. the model can be calibrated.

12 Future work

To get a more accurate and reliable result from the simulations the chipping process needs to be implemented into the model. Some ideas have been thought about during the Master Thesis work but because of lack of time it was never implemented into the model.

When the chipping process is implemented to the simulation model one can create a number of disc cutters and link them together to a real tunnel boring machine. If the rock parameters are set to a known value from a test in the literature, the performance of the simulation model can be evaluated. Then the model can be tuned in and be used for the early stage in the design and development process.

13 References

- Gertsch, L., Gertsch, R., Rostami, J. (2002): Rock Fragmentation by disc cutter, a critical review and an update. *Proceedings of the North American Rock Mechanics Symposium (NARMS) – Tunnelling Association of Canada (TAC) Meeting*. Toronto, Canada, 2002, 9 pp.
- Gertsch, L., Gertsch, R., Rostami, J. (2007): Disc cutting tests in Colorado Red Granite: Implications for TBM performance prediction. *International Journal of Rock Mechanics & Mining Sciences*, No. 44, 2007, pp. 238-246.
- Hongyuan, L. (2003): *Numerical Modelling of the Rock Fracture Process under Mechanical Loading*. Ph.D. Thesis. Department of Civil and Mining Engineering, Division of Rock Engineering, Luleå University of Technology, 2003:04, Luleå, Sweden, 2003, 505 pp.
- Lindqvist, P-A., Rånman, K. E., (1980): *Mechanical Rock Fragmentation – Chipping under a disc cutter*. Diss. Division of Mining and Rock Excavation, University of Luleå, 1980:59, Luleå, Sweden, 1980, 38 pp.
- Lindqvist, P-A. (1982): *Rock Fragmentation by Indentation and Disc Cutting*. Ph.D. Thesis. Department of Mining and Rock Excavation, University of Luleå, 1982:20, Luleå, Sweden, 1982, A1-A26 pp.
- Nilsen, B., Ozdemir, L. (1993): Hard Rock Tunnel Boring Prediction and Field Performance, Chapter 52. *RETC Conference Proceedings, Boston*.
- Ozdemir, L., Rostami, J. (1993): A new model of for performance prediction of hard rock TBM's. *Proceedings of Rapid Excavation and Tunnelling Conference, Boston*. pp. 793-809.
- Rostami, J., Ozdemir, L., Nilson, B. (1996): Comparison Between CSM and NTH Hard Rock TBM Performance Prediction Models. *ISDT1996, Las Vegas*.
- Rostami J. (1997): *Development of a Force Estimation Model for Rock Fragmentation with Disc Cutters Through Theoretical Modelling and Physical Measurement of Crushed Zone Pressure*. Ph.D. Thesis. Mining Engineering. Colorado School of Mines, Colorado, USA, 1997, 273 pp.
- Roxborough, F. F., Phillips, H. R. (1975): Rock Excavation by Disc Cutter. *Int. J. Rock. Mech. Min. Sci. & Geomech. Abstr.*, Vol. 12, 1975, pp. 361-366.
- Sanio, H. P (1985): Prediction of the Performance of Disc Cutters in Anisotropic Rock. *Int. J. Rock. Mech. Min. Sci. & Geomech. Abstr.*, Vol. 22, No. 3, 1985, pp. 153-161.
- Shaoquan, K. (1995): *Some Basic Problems in Rock Breakage by Blasting and by Indentation*. Ph.D. Thesis. Division of Mining Engineering, Luleå University of Technology, 1995:180D, Luleå, Sweden, 1995.

Snowdon, R. A., Ryley, M. D., Temporal, J. (1982): A Study of Disc Cutting in Selected British Rocks. *Int. J. Rock. Mech. Min. Sci. & Geomech. Abstr*, Vol. 19, 1982, pp. 107-121.

Online documentation, Adams 2008 r1

Appendix A

In Appendix A a simplified approach to the modelling procedure is presented. This is the way the simulation model presented in this Master Thesis has come into being. The Master Thesis is made through a crawl, walk and run approach. In appendix A the modelling of a wheel on a flat ground is considered.

A Modelling of a rolling wheel on a flat surface

A.1 Rolling wheel model

To get a better understanding and knowledge of Adams modelling and to make sure that the model works as expected a simple wheel was modelled. The wheel had the shape of a disc with sharp edges and was rolling on a flat surface. The wheel was attached to a fork, added to a vertical cylinder. The vertical cylinder was attached to a horizontal cylinder, see Figure 39.

A.1.1 Markers

A marker is used in Adams whenever a certain direction or position needs to be specified. It can for example specify where a geometry needs to be anchored to the part or where the centre of mass of the part is. When building a model, a marker defining the global origin will always be attached. This marker also says where the global directions are. All new markers will automatically have their positions and directions expressed in the global reference system.

A.1.2 Joints

Between the fork and the vertical cylinder there was a revolute joint, which means that the wheel was free to rotate in that direction. There was a cylindrical joint between the vertical and horizontal cylinder, the reason for that was to be able to steer the wheel. The horizontal cylinder was then jointed to the ground with a translational joint. This means that the horizontal cylinder did not rotate around the vertical cylinder. The translational joint can be replaced by a planar joint for example, keeping the distance to the ground constant but is able to rotate around the vertical cylinder.

When creating a joint two markers will be created. They are called the I- and J-marker. The I-marker belongs to the first part and the J-marker belongs to the second part of the two parts jointed together. For example, the revolute joint between the fork and the wheel, one marker will be on the fork and one marker on the wheel. The two markers will have their z-axis parallel and they will rotate around that axis.

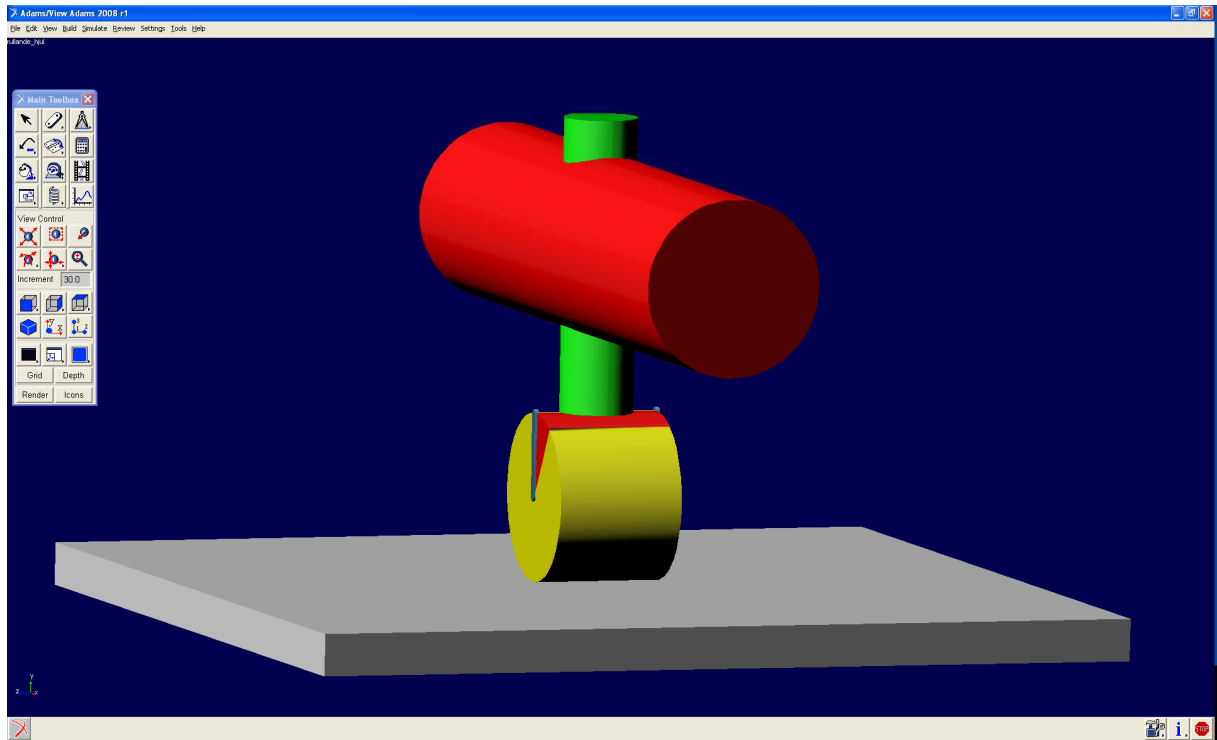


Figure 39 The wheel and the flat surface modelled in ADAMS

A.1.3 General force

The contact between the wheel and the ground was modelled with a six component general force. The same type of general force will be used later when building the simulation model for the disc cutter. The general force was attached to the centre of the wheel with its reference marker attached to the ground. This means that the force will act on the centre of the wheel with its components in the directions of the axis of the reference marker.

A.1.4 Directions

The directions in which the forces will act and the moment will act around are illustrated in Figure 45, with the z-direction pointing upwards from the grey box and the x-z-plane on the top of the grey box that the wheel will roll on.

A.1.5 Markers

When creating a general force, three markers are created. One marker will be placed on the action part, called the I-marker, one marker on the reaction part, J-marker, and one reference marker. The reference marker is in this case placed on the ground, which means that the components will be expressed in a system that is not moving with the wheel. This reference marker could be placed on any part of the model. The reaction part will in this case be the ground and the action part will be the wheel. Both the I- and J-markers will be placed in the centre of the wheel but the J-marker belongs to the ground and will not rotate with the I-marker. The I-marker will rotate with the wheel.

A.2 Forces and moments

A.2.1 Impact force

When the wheel touches the ground a normal force will appear. This normal force is modelled with the Adams function *IMPACT*. The *IMPACT* function in Adams calculates the impact force for when the wheel touches the ground. The function is

$$IMPACT = \begin{cases} \text{Max}(0, k(x_1 - x)^e - STEP(x, x_1 - d, c_{\max}, x_1, 0)\dot{x}) & x < x_1 \\ 0 & x \geq x_1 \end{cases} \quad (1)$$

where

x	Distance from the centre of the wheel to the ground, i.e. the y -coordinate of the general force in the global coordinate system used in the model
\dot{x}	Time derivative of the distance
x_1	Distance in the global y -direction in the model for when the wheel gets in contact with ground
k	Stiffness of the boundary surface interaction
e	Exponent of the force damping characteristics
c_{\max}	Maximum damping coefficient
d	Penetration for when full damping is applied

The step function approximates the Heaviside step function with a cubical polynomial. It has continuous first derivatives and its second derivatives are discontinuous at $x=x_0$ and $x=x_1$, see Figure 40.

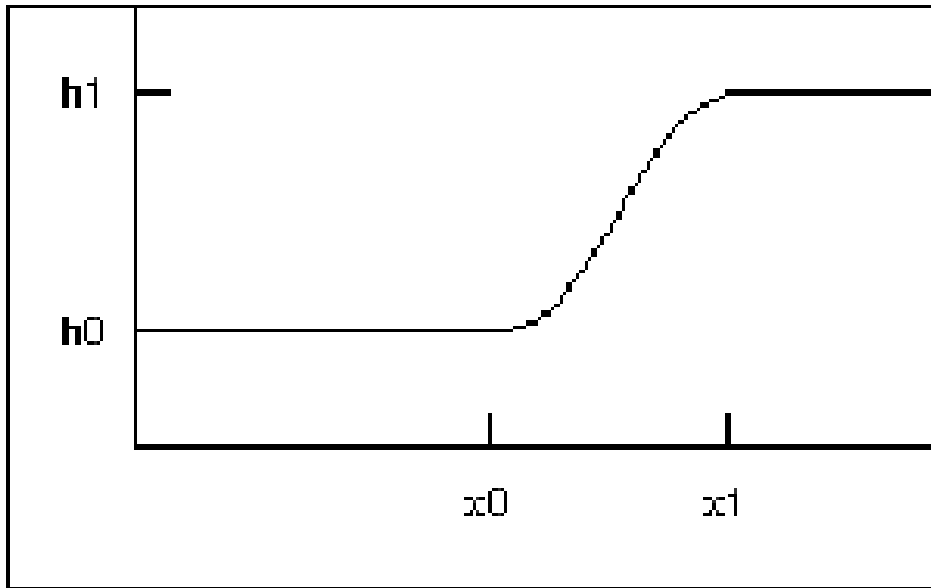


Figure 40 The step function used in the Adams function IMPACT. Online documentation, Adams 2008r1

The IMPACT function never returns a negative force. As can be seen in the function expression, equation (1), it only generates a force when the wheel is in contact with ground. The positive direction is the positive z -direction in reference system of the general force. The distance from the centre of the wheel to the ground is measured using the Adams built in function DZ and velocity is measured with the Adams function VZ. When measuring the distance, one should specify the marker to measure to, the marker to measure from and the marker to use as a reference. The velocity is measured in a similar way, but then one could also specify a reference frame to take the time derivative of the displacement vector. The I-marker for the general force, placed in the centre of the wheel is used as the marker to measure the distance to. The reference marker of the general force is used both as the marker to measure from and the marker to use as a reference, i.e. the coordinate system to measure in. The velocity is measured to the J-marker for the joint between the fork and the wheel, on the fork. This marker is placed at the centre of the wheel on the same place as the I-marker of the general force. The reference system for the general force is used as the reference frame for the time derivatives of the displacement vector. Since the stiffness multiplied by the penetration always will yield a positive force, the force from the damping factor will work against the motion. At first, when it moves into the ground it will be positive, and then the velocity will change sign and the force from the damper will be negative. The damping factor as a function of the penetration can be seen in Figure 41.

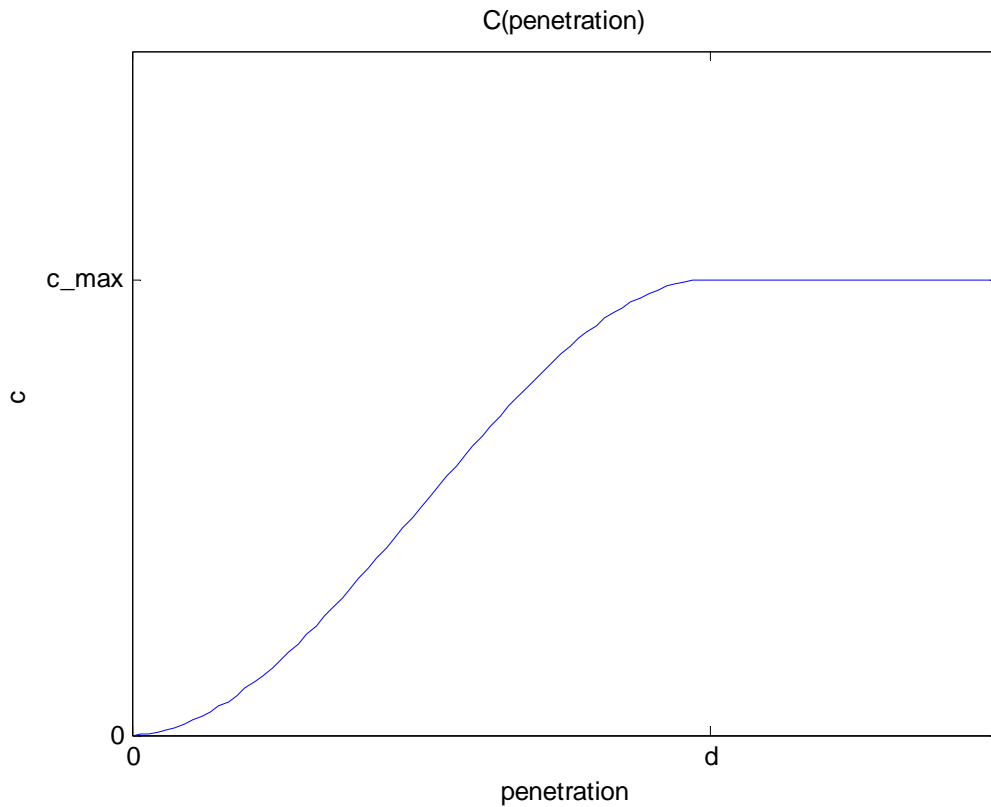


Figure 41 The damping factor as a function of the penetration

A.2.2 Friction force

A rolling condition is attached to the model, to see if the wheel is rolling or sliding. The rotational velocity of the wheel is measured in the joint between the fork and the wheel. The translational velocities of the wheel are measured in the reference system of the general force. A local coordinate system is then attached to the centre of the wheel for the simplicity of calculations. The local coordinate system can be seen in Figure 42. The z-axis has the same direction, which means that the x-y-planes are parallel.

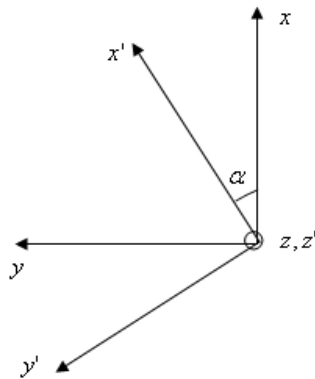


Figure 42 The orientation of the local coordinate system

Then the translational velocities are transformed to the new local coordinate system using a transformation matrix. The prime indicates the new local coordinate system. This transformation only takes the rotation around the z-axis into account. When modelling the disc cutter all three rotations will be taken into account. The transformation is made as:

$$\begin{bmatrix} x' \\ y' \\ z' \end{bmatrix} = \begin{bmatrix} \cos(\alpha) & \sin(\alpha) & 0 \\ -\sin(\alpha) & \cos(\alpha) & 0 \\ 0 & 0 & 1 \end{bmatrix} \begin{bmatrix} x \\ y \\ z \end{bmatrix} \quad (2)$$

And

$$\begin{bmatrix} x \\ y \\ z \end{bmatrix} = \begin{bmatrix} \cos(\alpha) & -\sin(\alpha) & 0 \\ \sin(\alpha) & \cos(\alpha) & 0 \\ 0 & 0 & 1 \end{bmatrix} \begin{bmatrix} x' \\ y' \\ z' \end{bmatrix} \quad (3)$$

where

- α Angle of rotation between the two coordinate systems
- x X-component in the global reference system
- y Y-component in the global reference system
- z Z-component in the global reference system

- x' X-component in the new local coordinate system
- y' Y-component in the new local coordinate system
- z' Z-component in the new local coordinate system

The angle of rotation between the two coordinate systems is measured with the Adams function YAW. The two markers used are the newly introduced marker attached to the fork but located in the centre of the wheel, and the reference marker of the general force. This means that the pitch angle is measured of the marker's rotation in the reference coordinate system.

The difference between the translational velocity and the rotational velocity multiplied with the radius of the wheel is then calculated. If the difference is zero, the wheel is rolling, otherwise is it sliding. A friction coefficient is calculated using this difference in velocity. When the friction coefficient is calculated the friction force can be determined. The friction force is working in the direction of the velocity vector calculated with the velocity difference in the x-direction due to sliding and the velocity in the z-direction, in the local coordinate system. The velocity difference is calculated as:

$$\Delta v = v_x' - \omega_z r \quad (4)$$

where

- Δv Difference in velocity
- v_x' Velocity in the x'-direction
- ω_z Angular velocity around the z-axis
- r Radius of the wheel

The minus sign between the velocity in the x-direction and the rotational velocity in the y-direction comes from the directions of the axes, we want the difference in velocity. The velocity in the direction that the friction force will work is calculated as:

$$v_{fr} = \sqrt{\Delta v^2 + v_y'^2} \quad (5)$$

where

v_{fr} Magnitude of the velocity in the direction of the friction force

Δv Difference in velocity

$v_{y'}$ Velocity in the y' -direction

The different velocities and the rotation of the wheel can be seen in Figure 43. The friction velocity will always have the same component in the local y -direction as the real translational velocity of the wheel in the same direction.

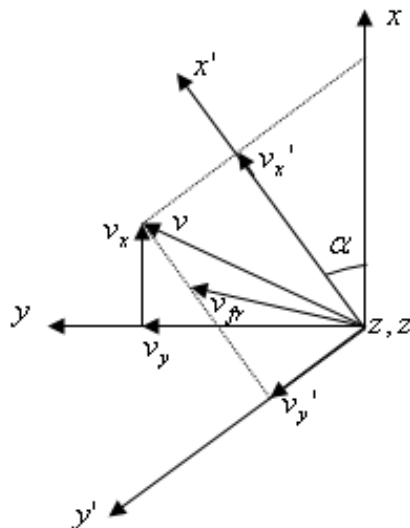


Figure 43 The coordinate systems with the different velocity components

When the friction velocity is calculated the friction coefficient can be calculated. The friction coefficient is calculated using a step function. The step function for calculating the friction coefficient can simply be expressed as:

$$\begin{aligned}
 a &= h_1 - h_0 \\
 \Delta &= \frac{x - x_0}{x_1 - x_0} \\
 STEP &= \begin{cases} h_0 & x \leq x_0 \\ h_0 + a\Delta^2(3 - 2\Delta) & x_0 < x < x_1 \\ h_1 & x \geq x_1 \end{cases}
 \end{aligned} \tag{6}$$

Using the friction parameters this will be:

$$\begin{aligned}
 a &= 2\mu \\
 \Delta &= \frac{v_{fr} + v_s}{2v_s} \\
 STEP &= \begin{cases} -\mu & v_{fr} \leq -v_s \\ a\Delta^2(3 - 2\Delta) & -v_s < v_{fr} < v_s \\ \mu & v_{fr} \geq v_s \end{cases}
 \end{aligned} \tag{7}$$

The friction model is simplified and does not contain the stiction friction coefficient, which would have given a higher friction force for the specific stiction velocity. Stiction is the phase just before sliding and is the maximum friction force. The friction coefficient distribution used in this model can be seen in Figure 44.

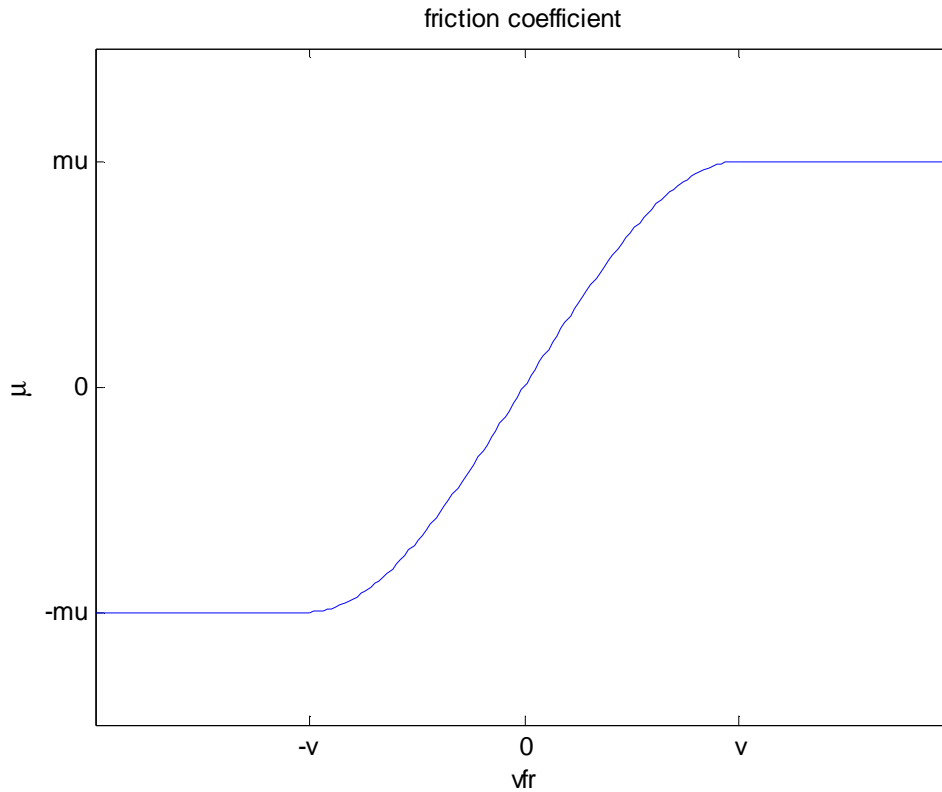


Figure 44 The friction coefficient as a function of the velocity

When the friction coefficient is determined the friction force can be calculated as the friction coefficient multiplied with the normal force as:

$$F_{fr} = F_n \mu \quad (8)$$

where

F_{fr} Friction force

F_n Normal force

μ Friction coefficient

The force components can then be calculated in the local coordinate system, by multiplying the friction force with the velocity in that direction divided by the magnitude of the velocity in the direction of the friction force. This is done as:

$$F_x' = \frac{\Delta v}{v_{fr}} F_{fr} \quad (9)$$

$$F_y' = \frac{v_y'}{v_{fr}} F_{fr} \quad (10)$$

where

F_x' Force in the x -direction in the local coordinate system

F_y' Force in the y -direction in the local coordinate system

v_{fr} Magnitude of the velocity in the direction of the friction force

Δv Difference in velocity

F_{fr} Friction force

The forces are acting at the contact between the wheel and ground. When they are moved to the centre of the wheel they give rise to added moments. The moments are calculated in the local coordinate system at first and will then be transformed to the global reference system at a later stage. The moments are calculated as:

$$\begin{aligned} T_x' &= F_y' R \\ T_y' &= -F_x' R \\ T_z' &= 0 \end{aligned} \quad (11)$$

Where

T_x' Moment around the local x -axis

T_y' Moment around the local y -axis

T_z' Moment around the local z -axis

R Radius of the wheel

The distance between the centre of the wheel to the contact point on the ground will always be positive. The forces and moments in the local coordinate system will then be transformed back to the global reference system using the transformation matrix introduced before. Since the global and local z -axes are not transformed the

components will be the same. The transformation yields the following forces and moments:

$$\begin{aligned}
 F_x &= F_x' \cos(\alpha) - F_y' \sin(\alpha) \\
 F_y &= F_x' \sin(\alpha) + F_y' \cos(\alpha) \\
 F_z &= F_N \\
 T_x &= T_x' \cos(\alpha) - T_y' \sin(\alpha) \\
 T_y &= T_x' \sin(\alpha) + T_y' \cos(\alpha) \\
 T_z &= T_z'
 \end{aligned}
 \tag{12}$$

When the forces and moments are calculated they are attached in the centre of the wheel, the I-marker of the general force.

A.2.3 Subroutine

All the measurements and calculations described above are made in a subroutine. A subroutine is a more general and flexible way of writing functions in Adams. There are subroutine templates available in Adams to use when writing a user written subroutine. In this case, the template for a GFOSUB is used, general force subroutine. In the beginning of the subroutine the input and output parameters are stated.

The subroutines are written in the computer programming language Fortran 77. The parameters from the model such as wheel radius, wheel width, friction coefficient, stiffness, damping, friction velocity and the distance for full damping are stored in a vector and are then sent to the subroutine. All the input data are then defined, and a number of checks are made to see that the correct number of inputs are sent to the subroutine and that the vector has the correct number of elements and that the correct number of parameters are sent to the subroutine. These parameters are in this case the a branch number, an ID-serie, the Adams ID-number of the I-marker of the general force, the Adams ID-number for the reference marker of the general force, the Adams ID-number of the I-marker of the joint between the wheel and the fork, the Adams ID-number of the J-marker of the joint between the wheel and the fork and the ID-number of the array. Each marker has a Adams ID-number.

When that is made all the measurements can be made. The first measurements to do are ones required to calculate the free height of the impact function. That is done to know if the wheel is in contact with the ground or not, if it is not in contact then the forces can be set to zero leave the subroutine for the next step. When the wheel is in contact with ground, the measurements described above are made and the forces and moments are calculated and attached to the centre of the wheel. The directions of the general force can be seen in Figure 45.

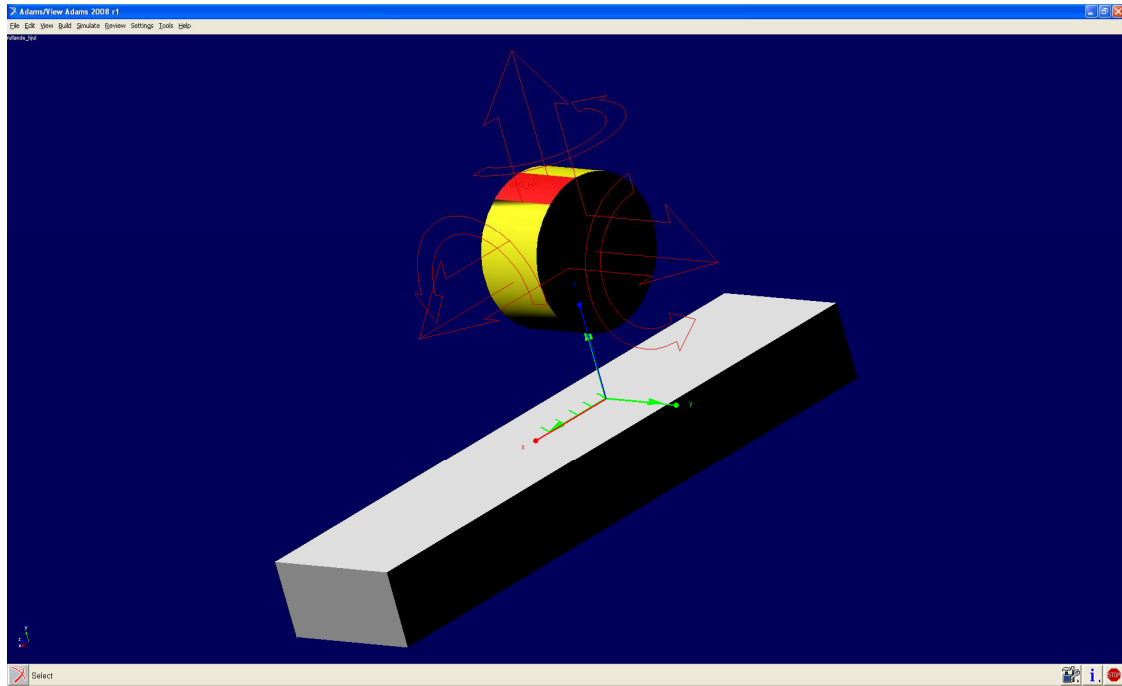


Figure 45 The directions of the components of the general force and the reference coordinate system, the x-axis is red, the y-axis is green and the z-axis is blue

Appendix B

In Appendix B the simplified model to update the deformation of the ground is presented.

B Ground deformation model

B.1 Introduction

To be able to simulate rock cutting with a disc cutter the rock fragmentation process must be modelled. The ground will be modelled using the mesh described in Chapter 5. This chapter is about the first simple model of the ground deformation, to learn the tools that will be used on the rock fragmentation later.

B.2 Force calculation

The force will be modelled as a general force attached to the centre of the wheel as in Appendix A. The difference from that case is that now the rock surface matrix is used to describe the ground instead of the z-coordinate zero. The rock surface matrix is a matrix with all the z-coordinates from each node from a triangular mesh stored in each position of the matrix. The matrix is thoroughly described in Chapter 5.

B.2.1 Mean surface

Since the IMPACT function described in Appendix A, Chapter A.2.1 will be used to calculate the force acting in the z-direction of the reference marker of the general force, a mean value of the height of the ground must be calculated. The position of the centre of the wheel is measured using the ADAMS built in measure functions DX, DY and DZ. When the position is known one can sweep over the area just beneath the wheel and calculate the z-coordinates as a function of the x- and y-coordinates of the wheel surface. The wheel surface is divided into a number of small elements where the z-coordinate in the centre of each small element is calculated. The area of the rock surface under the wheel is illustrated in Figure 46, where the distances and coordinates calculated below are defined.

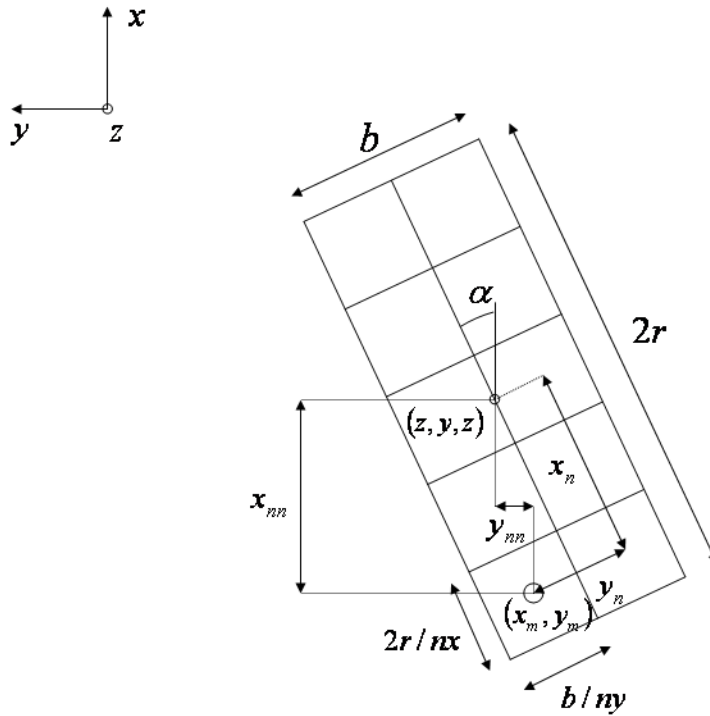


Figure 46 The distances for the calculation of the mean surface

The distance from the centre of the wheel to the centre of each small element that the area under the wheel is divided into, in x- and y-direction, in the local coordinate system is calculated according to equation (13) and (14).

$$x_n = r + \left(\frac{2r}{nx}\right)(L - 0.5) \quad (13)$$

$$y_n = \frac{b}{2} + \left(\frac{b}{ny}\right)(K - 0.5) \quad (14)$$

The coordinates are then transformed to the reference system according to the following transformation equation (15).

$$\begin{aligned} x_{mn} &= x_n \cos(\alpha) - y_n \sin(\alpha) \\ y_{mn} &= x_n \sin(\alpha) + y_n \cos(\alpha) \end{aligned} \quad (15)$$

Finally the coordinate of the centre of the small element can be calculated according to the equations below, equation (16) and (17).

$$x_m = x - x_{mn} \quad (16)$$

$$y_m = y - y_{mn} \quad (17)$$

When the position of the centre of the small element is determined, here y_m and x_m , the four surrounding nodes can be calculated. This is calculated according to equations (19) to (24).

$$kk_x = INT\left(\frac{x_m - x_{\min}}{dx}\right) \quad (18)$$

$$kk_y = INT\left(\frac{y_m - y_{\min}}{dy}\right) \quad (19)$$

$$k_{x1} = kk_x + 1 \quad (20)$$

$$k_{y1} = kk_y + 1 \quad (21)$$

$$k_{x2} = k_{x1} + 1 \quad (22)$$

$$k_{y2} = k_{y1} + 1 \quad (23)$$

where

$INT(A)$	Rounds A to the nearest integer less than or equal to A
kk_x	Start coordinate in the x-direction
kk_y	Start coordinate in the y-direction
x_m	Actual position of the centre of the element in the x-direction
y_m	Actual position of the centre of the element in the y-direction
x_{\min}	Coordinate of node one in the x-direction
y_{\min}	Coordinate of node one in the y-direction
dx	Element length in the x-direction
dy	Element length in the y-direction
k_{x1}	Lowest node number in the actual element in the x-direction
k_{y1}	Lowest node number in the actual element in the y-direction
k_{x2}	Highest node number in the actual element in the x-direction

k_{y2} Highest node number in the actual element in the y-direction

When the four surrounding nodes in the rock surface matrix are determined one can determine whether the centre of the node is located in the upper or lower element. At first, the distance from the centre of the small element to the k_{x1} and k_{y1} node must be calculated. This distance is calculated according to equations (24) and (25).

$$xx1 = x - (kk_x \cdot dx + x_{\min}) \quad (24)$$

$$yy1 = y - (kk_y \cdot dy + y_{\min}) \quad (25)$$

These distances are used to determine whether the centre of the disc cutter is in the upper or the lower element, see Figure 47 and Figure 48. The actual element is determined as:

$$\begin{aligned} \text{if } xx1 < yy1 &\rightarrow \text{upper} \\ \text{else } &\text{lower} \end{aligned} \quad (26)$$

When the actual element in the rock surface matrix where the centre of the small element is located is determined one can interpolate the z-coordinate in the rock surface for the point of interest. This interpolation is done according to the following equations, see also Section 3.3.1 for a further description of the calculations. When the centre of the small element is located in a lower element in the rock surface the z-coordinate is calculated using the following equation, equation (27).

$$z(x_m, y_m) = z_{rock}(k_{x1}, k_{y1}) + \frac{dz}{dx} xx1 + \frac{dz}{dy} yy1 \quad (27)$$

The figure below, Figure 47, shows the situation when the point of interest is located in the lower element.

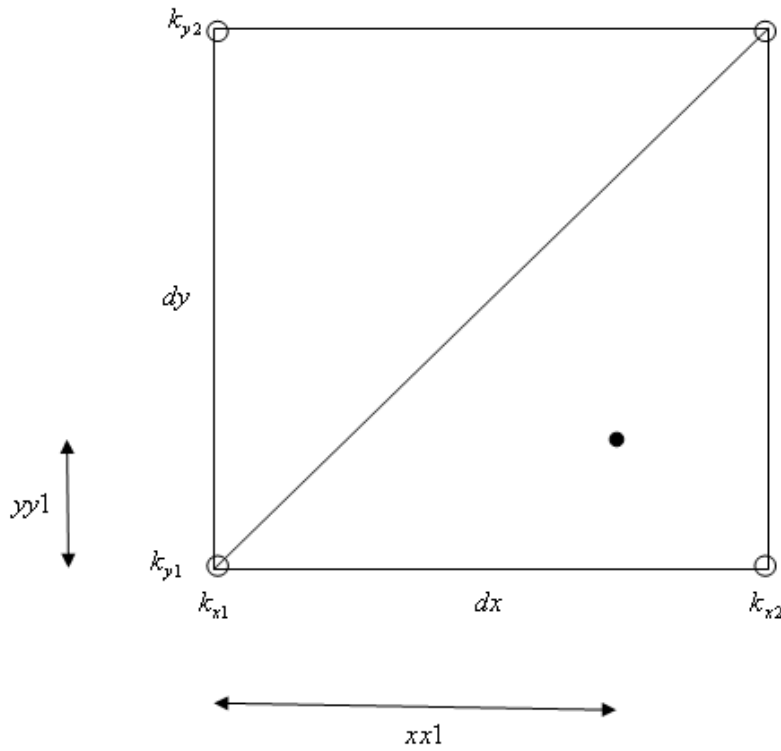


Figure 47 The actual position in the lower element

When the centre of the small element is located in the upper element in the rock surface the z-coordinate is calculated using the following equation.

$$z(x_m, y_m) = z_{rock}(k_{x1}, k_{y1}) + \frac{dz}{dx} xx1 + \frac{dz}{dy} yy1 \quad (28)$$

The actual position in the upper element can be seen in Figure 48.

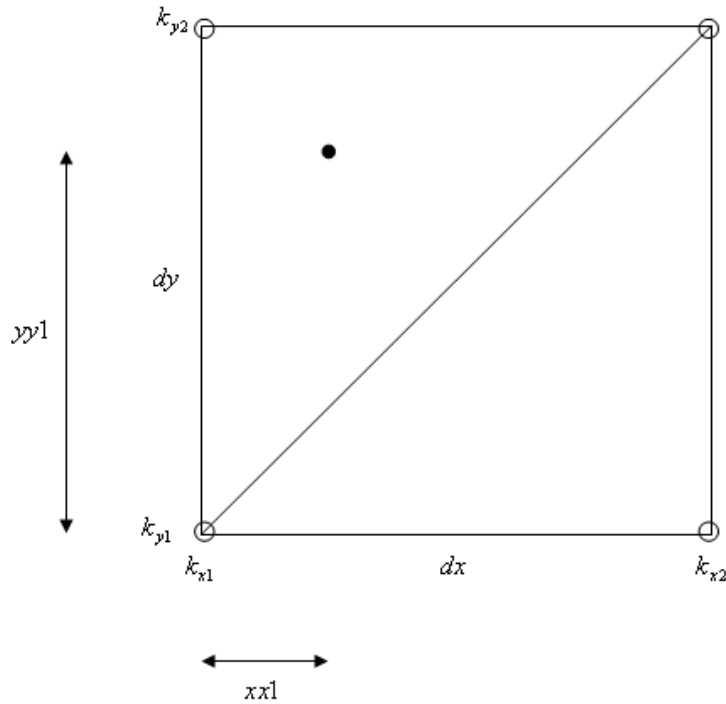


Figure 48 The actual position in the upper element

The mean surface under the cutter is calculated using the z-coordinate for the centre of each small element multiplied with the area of each small element. The area of each element is calculated as equation (29):

$$A_{element} = \frac{2r}{nx} \cdot \frac{b}{ny} \quad (29)$$

The total area of the whole surface under the wheel is calculated according to equation (30).

$$A_{tot} = b \cdot 2r \quad (30)$$

The mean surface under the wheel is calculated as the sum of the z-coordinate of the centre of each small element multiplied with the area of each small element, this is then divided by the total area of the surface under the wheel. This is done according to equation (31).

$$z_{mean} = \frac{\sum_{i=1}^n (A_{element} \cdot z(x_m, y_m))}{A_{tot}} \quad (31)$$

Where

i Small element number

n Total number of small elements

B.2.1 Impact function

The mean value of the z-coordinate for the rock surface under the wheel will be used to calculate the distance from the centre of the wheel to the ground. This distance will be used in the ADAMS built in function IMPACT to calculate the force working on the wheel. The force is calculated in the same way as in Chapter A.2.1, but now with a varying distance to the ground instead of $z=0$ as used then.

B.2.2 Deformation

When the wheel is rolling on the rock surface it penetrates into it. When it penetrates the rock surface matrix must be updated with the new deformed z-coordinate for the nodes that has been penetrated.

B.2.3 Penetration

The penetration of the wheel into the ground will be calculated using a loop that will be made over all the elements in the rock surface matrix. The coordinate in the x- and y-direction will be calculated for the nodes, according to equation (34) and (35). The calculations made for one node can be seen in Figure 49.

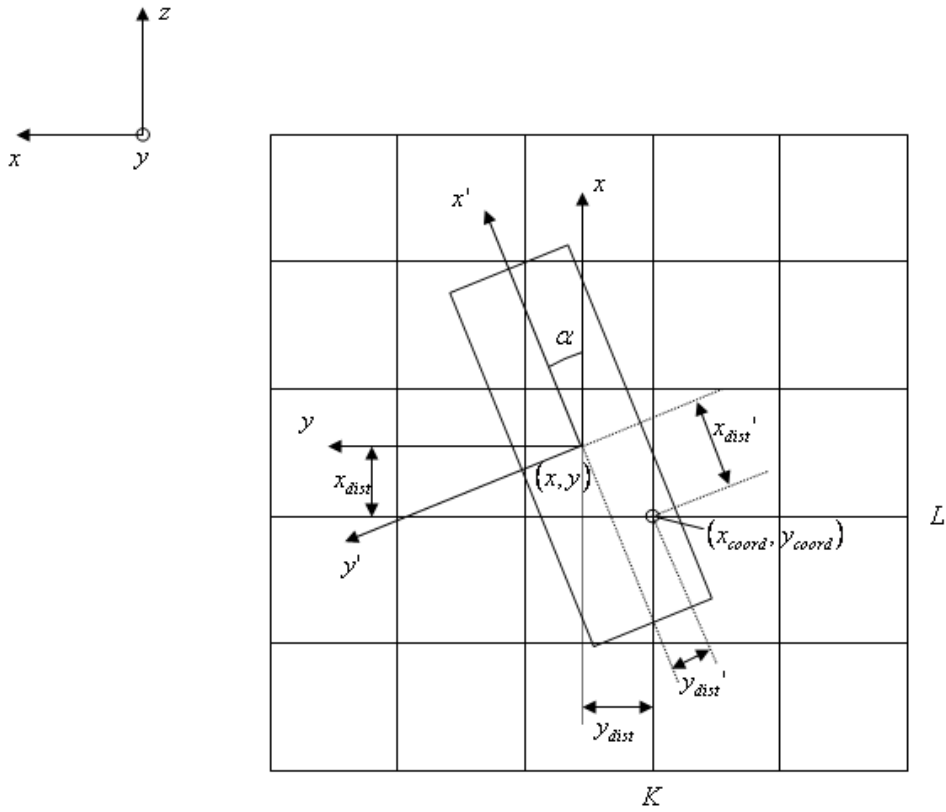


Figure 49 The distances and angles when calculating the penetration of each node in the rock surface matrix

$$x_{coord} = x_{min} + dx \cdot (L - 1) \quad (32)$$

$$y_{coord} = y_{min} + dx \cdot (K - 1) \quad (33)$$

The coordinates of the node of interest will then be used to calculate the distance from the centre of the wheel to the specific node. The distance from the node to the centre of the wheel is calculated using the equation below.

$$x_{dist} = x_{coord} - x \quad (34)$$

$$y_{dist} = y_{coord} - y \quad (35)$$

When the distance is calculated it will be transformed into the local coordinate system according to equation (36), to be able to turn the wheel in different directions in the rock surface.

$$\begin{bmatrix} x_{dist}' \\ y_{dist}' \end{bmatrix} = \begin{bmatrix} \cos(\alpha) & \sin(\alpha) \\ -\sin(\alpha) & \cos(\alpha) \end{bmatrix} \begin{bmatrix} x_{dist} \\ y_{dist} \end{bmatrix} \quad (36)$$

Now we make a check to see if the node we are looping through right now is located in the area under the wheel or not. If the absolute value of the transformed distance in

the local x-direction is smaller than the wheel radius, and if the absolute value of the transformed distance in the y-direction is smaller than half of the wheel width, then the node is located under the area of the wheel. This is done according to:

$$\begin{array}{l} \text{if } x_{dist}' < r \text{ then} \\ y_{dist}' < b/2 \text{ then} \end{array} \text{inside} \quad (37)$$

If the node of interest is located inside the area of the wheel the z-coordinate of the point of the wheel corresponding to the position of the node is calculated. The z-distance for the point on the wheel surface from the centre of the wheel is calculated according to:

$$H = \sqrt{r^2 - x_{dist}'^2} \quad (38)$$

The calculation of the distance from the centre of the wheel to the point of the wheel edge and the z-coordinate for the point of the wheel edge can be seen in Figure 50.

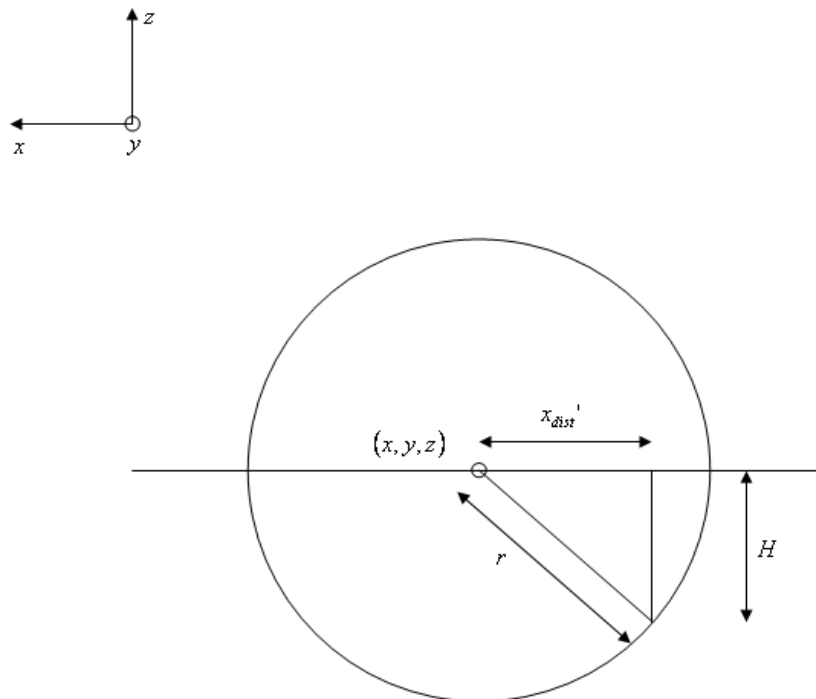


Figure 50 Definition of the z-coordinate for each point in the loop over the edge of the wheel

The last check to make is that if the point on the wheel has a smaller z-coordinate than the corresponding point on the rock surface. The z-coordinate for the point on the wheel edge is calculated as the z-coordinate for the centre of the wheel minus the

distance in the z-direction from the centre of the wheel to the point on the wheel edge, according to equation (39).

$$z_{coord,wheel} = z_{coord,wheelcentre} - H \quad (39)$$

When the z-coordinate of the point on the wheel surface is calculated one can check if the point has penetrated into the rock according to equation (40).

$$\text{if } z_{coord,wheel} < z_{rock}(L, K) \text{ then penetration} \quad (40)$$

The depth of the penetration for a certain node in the rock surface mesh can be seen in Figure 51.

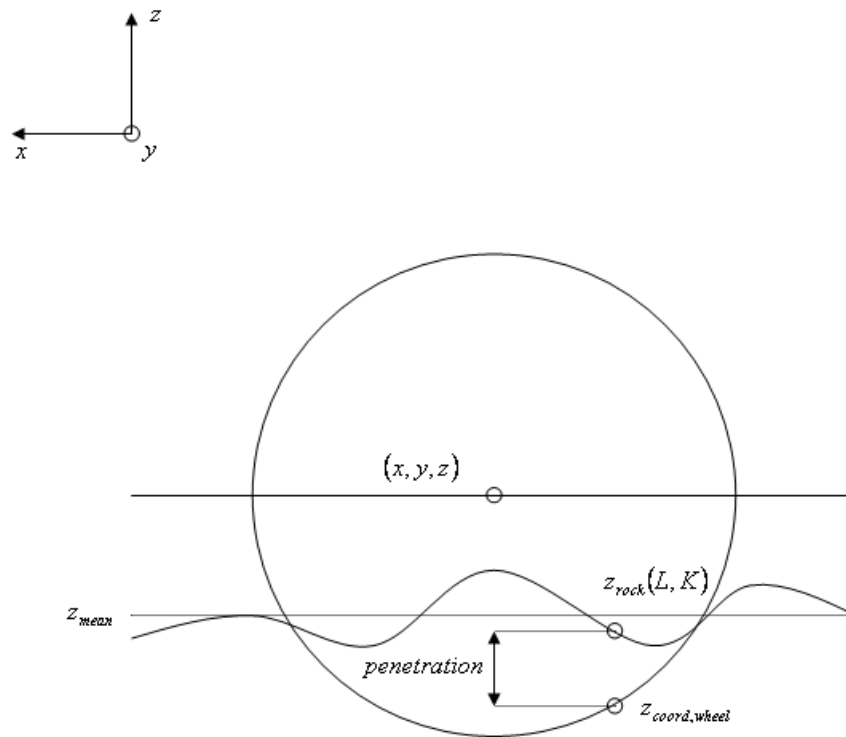


Figure 51 The penetration for each node in the rock surface matrix

B.3 Matrix update

If the point on the wheel surface has penetrated into the rock surface and created an inelastic deformation the rock surface matrix must be updated with a new z-value for that specific node. In this case half of the penetration into the rock surface has been seen as an inelastic deformation.

B.3.1 Temporary rock matrix

When there is an inelastic penetration into the rock surface causing a deformation of the rock a temporary rock matrix is created. From the temporary rock matrix a determined part of the z-value of the node of interest is removed, in this case half of the penetration depth. If the time step is successful the temporary rock matrix is copied to the rock matrix, but if the time step is not successful the temporary rock matrix will not be copied.

B.3.2 Time steps

If the time step is too long and the system can not be solved the length of the time step needs to be shortened. When this happens the temporary matrix will be replaced with the rock matrix since the temporary rock matrix is not valid when the time step is decreased and the simulation time decreases.